Monatsh Chem (2011) 142:659–680
DOI 10.1007/s00706-011-0467-9

REVIEW

Enantioselective synthesis of proline derivatives by 1,3-dipolar cycloadditions

Carmen Nájera · José M. Sansano

Received: 18 January 2011 / Accepted: 21 February 2011 / Published online: 18 March 2011

Abstract Research devoted to the synthesis of highly substituted prolines, which are hepatitis C virus inhibitors, using 1,3-dipolar cycloadditions (1,3-DC) of azomethine ylides is described. In the first part, a diastereoselective approach using an inexpensive lactate-derived acrylate as dipolarophile is described. In the second part, our efforts using simple and easily accessible chiral silver(I) and gold(I) complexes as catalysts for enantioselective synthesis of proline derivatives are reviewed. In this case, chiral phosphoramidites and binap have been used as privileged ligands. Parallel to these experimental results, considerable effort was dedicated to run semiempirical density functional theory (DFT) calculations to explain and justify the stereoselectivity of each process.

Keywords Antiviral activity · Chiral catalysts · Azomethine ylides · Cycloadditions · Prolines · Lewis acids

Introduction

Proline derivatives

Proline (**1**) and its derivatives constitute a very important family of natural or synthetic compounds with very interesting chemical and bioactive applications. Proline surrogates are of special interest given the key role of proline in nucleating the secondary structures, and hence the biological behavior of peptides. These rigid amino acids represent a powerful means to overcome their shortcomings, since limited conformational freedom often protects against proteolytic degradation and sometimes leads to improved selectivity and potency [1].

In addition to this main application, they are also often used in structure–activity relationship (SAR) studies [1], synthesis of pyrrolidine core-based natural products [1–3], and even application of these small units as very efficient organocatalysts [4, 5]; for example, 4-hydroxyproline (**2**) (R = H) is the major component of the protein collagen, playing key roles in the increment of collagen stability. (−)-α-Kainic acid (**3**), (−)-domoic acid (**4**), and acromelic acid (**5**) belong to a family of kainoid natural neurotoxins, promoting potent stimulation of the central nervous system, brain damage, and neurological disorders (Fig. 1) [1]. In addition, synthetic molecules **6**–**9** have been identified as potent hepatitis C virus (HCV) inhibitors blocking the viral RNA-dependent RNA-polymerase [6]. Finally, the proline derivative **9** (GSK 625433), which is now in phase I trials, has shown potent selective activity against type 1a and 1b HCV polymerases. Moreover, proline (**1**) or its derivatives **2**, **10**, and **11** are suitable as new organocatalysts for asymmetric synthesis [4, 5].

A number of strategies devised for synthesis of proline derivatives [1–3, 7] involve: (a) α-functionalization of L-proline itself or other derivatives, (b) intramolecular cyclizations of chiral amino acids, and (c) formation of the pyrrolidine ring through 1,3-dipolar cycloaddition (1,3-DC) of azomethine ylides. The latter methodology is the most straightforward route for preparation of highly substituted prolines.

1,3-Dipolar cycloadditions of azomethine ylides

Since the publication of the first example of 1,3-DC by Huisgen in 1963 [8], many contributions have appeared

C. Nájera · J. M. Sansano (✉)
Departamento de Química Orgánica e Instituto de Síntesis Orgánica, Universidad de Alicante, Apdo. 99, 03080 Alicante, Spain
e-mail: jmsansano@ua.es

C. Nájera
e-mail: cnajera@ua.es

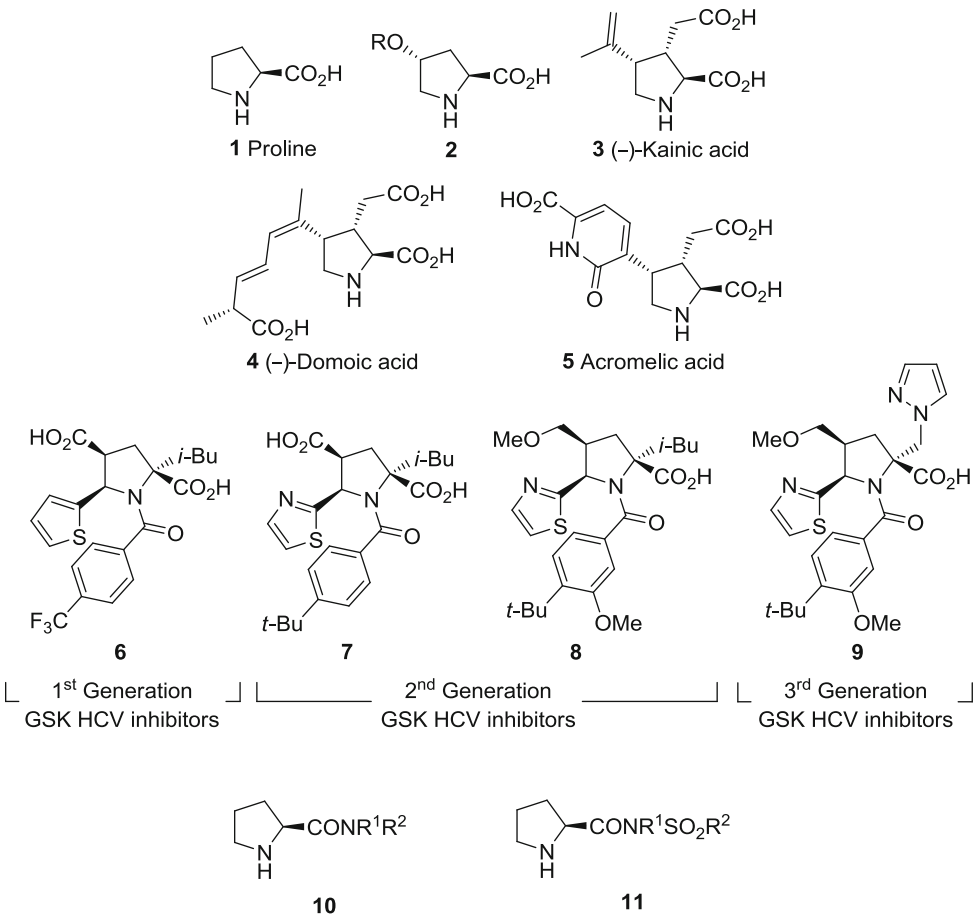

Fig. 1 Useful proline derivatives

(for recent reviews, see [9–12]). In recent years, azomethine ylides have become one of the most investigated classes of 1,3-dipoles, due to their cycloaddition chemistry (for recent reviews, see [9–23]).

The high reactivity of the azomethine ylides requires their generation in situ, which can be achieved through several routes. Whilst nonstabilized azomethine ylides are considered fleeting intermediates, the stabilized ones **14** or **15** possess longer lifetimes, allowing wider scope for cycloaddition. Nowadays, iminoesters **13** afford these 1,3-dipoles through a thermal 1,2-prototropy shift process or by base-promoted enolization followed by intramolecular chelation (Scheme 1). The latter process occurs under very mild reaction conditions, and the control of the geometry of the resulting metallodipole is extremely high. This feature, together with the frontier orbital theory (FOT)-justified regioselectivity, and the high *endo*- or *exo*-diastereoselectivity observed, make this generation of 1,3-metallodipoles much more attractive and useful in this particular organic synthesis area. The reaction of the dipole with the electrophilic alkene to give **16** occurs through a concerted process under thermal conditions, and, probably, in a stepwise manner (a Michael-type addition reaction followed by intramolecular cyclization) when a 1,3-metallodipole **15** is involved [13–23].

Standard 1,3-DC of the stabilized azomethine ylides **18**, easily prepared from iminoesters **17**, occurs with high-lowest

Scheme 1

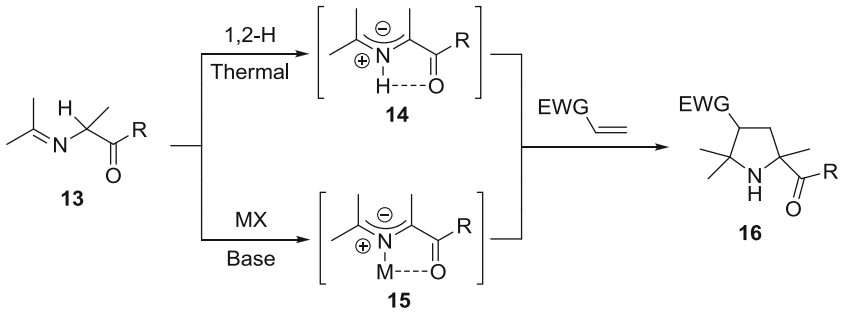

Scheme 2

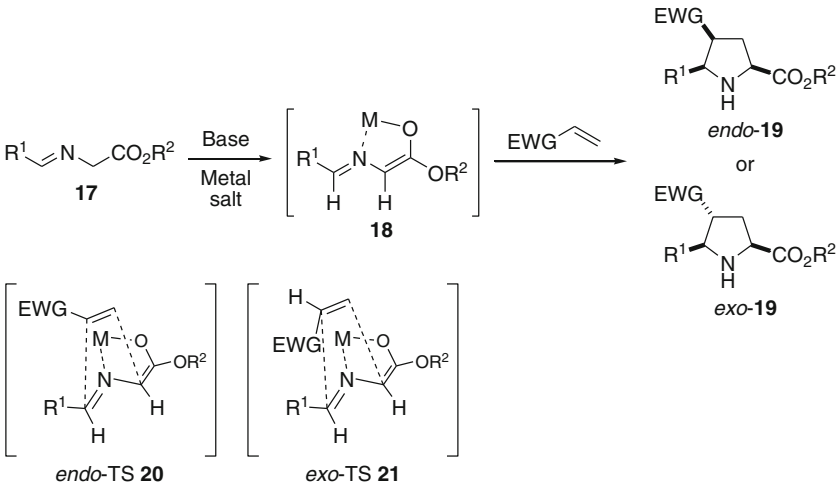

unoccupied molecular orbital (LUMO) alkenes under very mild reaction conditions, affording *endo*- or *exo*-cycloadducts **19** (Scheme 2). Stereoelectronic effects control the *endo*/*exo* ratio of the final product **19**. These *endo* and *exo* notations concern the two different approaches of the dipolarophile to the metal center. The *endo*-approach occurs when the electron-withdrawing group (EWG) that induces the Michael-type addition step is very close to the metal cation, favoring very weak coordination between them (*endo*-TS **20** in Scheme 2). However, in the *exo*-approach the EWG is oriented far away from the metal center, as depicted in *exo*-TS **21** in Scheme 2.

1,3-DC becomes extremely useful when all these aspects are focused on the design of an asymmetric process [13–23], where generation of up to four stereogenic centers can be unambiguously achieved in just one reaction step. Currently, nonracemic 1,3-DC can be efficiently achieved through diastereoselective strategies by employing chiral azomethine ylides or chiral dipolarophiles, and secondly, via enantioselective processes using chiral catalysts.

Herein, we describe the evolution of our research on the development of asymmetric methodologies for synthesis of biologically active HCV inhibitors **6**–**8**. In parallel, a wide study of the general scope of each of them will also be introduced.

Diastereoselective methods

In optically active azomethine ylides, the chiral information can be located at the EWG or at the imino group. However, achiral α-amino acid templates **23**–**25** have been described as azomethine ylide precursors, where the chiral domain is directly bonded to both functional imino and EWGs. The most recently reported chiral azomethine ylides are those derived from amines **22**–**25** [24–27] (Fig. 2) and aldehydes upon heating. In all cases, good chemical yields and moderate to good diastereoselectivity were obtained. At the end of the process, the chiral auxiliary must be separated from the pyrrolidine moiety. In this sense, for example, the Oppolzer's sultam fragment of precursor **22** could be easily recoverable under mild reaction conditions, yielding enantiomerically pure proline derivatives. By contrast, the chiral auxiliary was not removed in the case of the chiral iminoester **26** [28], which was the precursor of the silver metallodipole, and after completing the corresponding cycloaddition, the chiral *β*-lactam unit was employed for construction of more complex structures.

Alternatively, chiral electrophilic alkenes can be employed. In this option, the most recent examples anchor

Fig. 2 Some recent chiral 1,3-dipole precursors

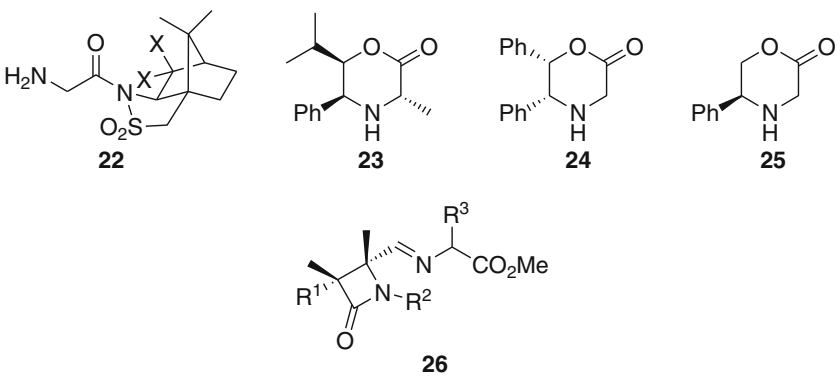

Fig. 3 Some recent chiral dipolarophiles

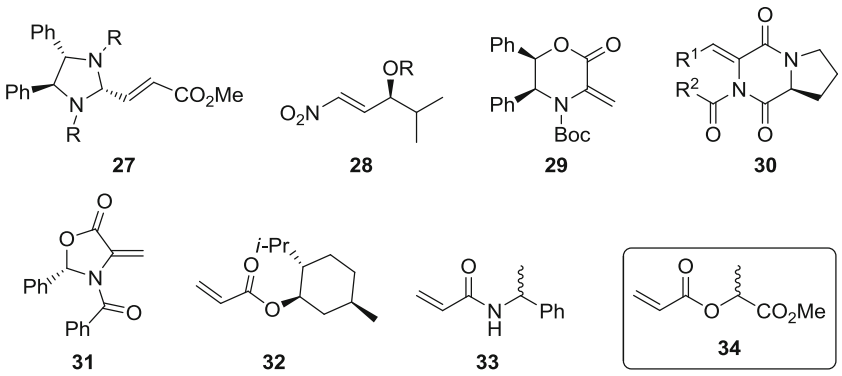

Scheme 3

the chiral information as substituent of the carbon–carbon double bond such as those occurring in **27** [29] and **28** [30], or at the EWG as, for example, in molecules **29**–**33** [31–35] (Fig. 3).

Enantiomerically enriched acrylates (*R*)- and (*S*)-**34**, employed in diastereoselective Diels–Alder reactions and in the synthesis of natural products and complex heterocycles [36, 37], were envisaged as chiral dipolarophiles in diastereoselective 1,3-DC. Firstly, we improved the synthesis of these enantiomerically enriched alkenes in a simple process involving esterification of the chiral lactic acid with acryloyl chloride in the presence of triethylamine and substoichiometric amounts of *N*,*N*-dimethylaminopyridine (DMAP) [38, 39]. This new procedure avoided use of the toxic and no longer commercially available carbon tetrachloride.

1,3-DC of (*S*)-**34** with metallo-azomethine ylides derived from iminoesters **35** efficiently proceeded under mild reaction conditions obtained after an optimization protocol, namely AgOAc (10 mol%), KOH (10 mol%) as base, in toluene at room temperature for 1 day (Scheme 3). For glycine-derived 1,3-dipoles, the influence of the ester group could be observed when the benzaldehyde iminoglycinates **35** (R^1 = H, R^3 = phenyl, 2-naphthyl) were allowed to react with the chiral alkene (*S*)-**34** (Table 1, entries 1–5). The reactions proceed quantitatively, and the best diastereoselectivities were achieved when the *t*-butyl esters were employed. One should note the higher diastereoselectivities exhibited by the methyl esters versus the analogous transformations performed with the isopropyl esters. Several α-substituted amino acids such as alanine, phenylalanine, and leucine were used for elaboration of the 1,3-dipole. In the reactions carried out with these α-branched 1,3-dipole precursors there was not a very significant difference, in terms of diastereoselectivity, between using methyl or *t*-butyl esters (see, for instance, Table 1, compare entries 6 and 7). So, all the reactions were performed in 2 days with the corresponding methyl esters, affording in all cases good chemical yields and good to excellent diastereoselectivities of the *endo*-cycloadducts **36**, especially for the reaction involving the phenylalanine derivative (R^3 = 2-thienyl, Table 1, entry 9). This excellent result encouraged us to design the key step for nonracemic synthesis of the first generation of the antiviral agent **6**. The reaction of the

Table 1 1,3-DC between chiral acrylate (*S*)-**34** and iminoesters **35**

Entry	R^1	R^2	R^3	Yield (%)[a]	*de* (%)[b]
1	H	Me	Ph	64	94
2	H	*i*-Pr	Ph	63	92
3	H	*t*-Bu	Ph	73	99
4	H	Me	2-Naphthyl	60	90
5	H	*t*-Bu	2-Naphthyl	70	99
6	Me	Me	Ph	65	90
7	Me	*t*-Bu	Ph	70	92
8	Bn	Me	2-Naphthyl	65	84
9	Bn	Me	2-Thienyl	65	95
10	*i*-Bu	Me	2-Thienyl	77	96
11	*i*-Bu	*i*-Pr	2-Thienyl	82	82
12	*i*-Bu	*t*-Bu	2-Thienyl	83	87

[a] Isolated yield after purification by flash chromatography

[b] Determined by chiral high-performance liquid chromatography (HPLC) columns

methyl, isopropyl, or *t*-butyl iminoleucinates (R^1 = *i*-Bu, R^3 = 2-thienyl) with the acrylate (*S*)-**34** occurred under the standard reaction conditions, affording good chemical yields and very good diastereoselectivity of the cycloadduct **36** (Table 1, entries 10–12). Once more, the methyl ester derivative was the most appropriate substrate, rather than isopropyl or *t*-butyl esters. In all of these examples, the *endo*/*exo* ratio observed by ^{1}H nuclear magnetic resonance (NMR) spectroscopy was higher than 98/2.

The absolute configurations of the *endo*-products **36** could be determined by X-ray diffraction analysis of the *N*-tosylated cycloadduct **37**, showing that the (*S*) absolute configuration of the lactate moiety induced a (2*R*,4*R*,5*S*) configuration in the pyrrolidine ring (Scheme 4).

According to this stereochemical arrangement, the acrylate (*S*)-**34** would be valuable for synthesis of (−)-**6**, whilst enantiomeric acrylate (*R*)-**34** would serve for preparation of the biologically more active compound (+)-**6**, although the activity of the racemic form is not negligible (Fig. 4). For this reason, we first undertook the synthesis of the antiviral agent (±)-**6** as shown in Scheme 5. The non-isolated cycloadduct obtained from the iminoester **35** (R^1 = *i*-Bu, R^2 = Me, R^3 = 2-thienyl) and methyl acrylate in the presence of AgOAc (10 mol%) was allowed to react with 4-(trifluoromethyl)benzoyl chloride in dichloromethane (DCM) for 2 days, yielding the corresponding amide **38** in 88% yield. The final product (±)-**6** was isolated in 68% yield after a combined hydrolytic process based on a treatment of tributyltin hydroxide required for elimination of the chiral auxiliary, followed by reflux of 1 M KOH/MeOH solution for hydrolysis of the ester group placed at the α-position of the proline (Scheme 5).

Synthesis of nonracemic antiviral agents had not been reported before these research studies, but the enantiomerically enriched samples were obtained through semipreparative chiral high-performance liquid chromatography (HPLC) columns [40, 41]. The preparation of both enantiomers (+)- or (−)-**6** was achieved using a very similar route starting from the iminoester **35** (R^1 = *i*-Bu, R^2 = Me, R^3 = 2-thienyl) and the more expensive acrylate (*R*)-**34** or the inexpensive acrylate (*S*)-**34**. These key steps afforded the *endo*-cycloadduct **35** in 77–78% chemical yield and 96% *de* (Table 1, entry 10). The amidation reaction and the double hydrolytic processes were identical to those described for the synthesis of the racemic antiviral agent (Scheme 6), obtaining overall yield of 68% from the cycloadduct **36**.

Scheme 4

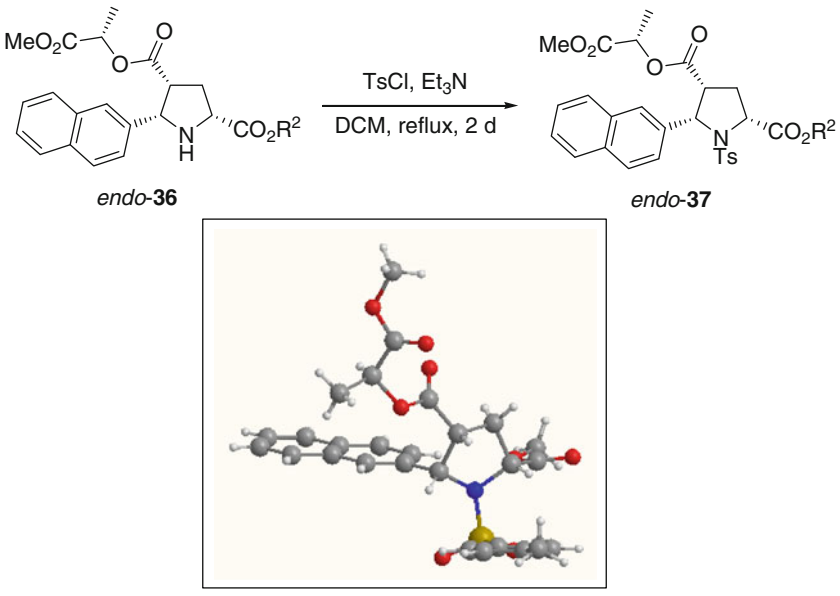

endo-**36** *endo*-**37**

Fig. 4 Biological activity of the most active first GSK generation of HCV inhibitors

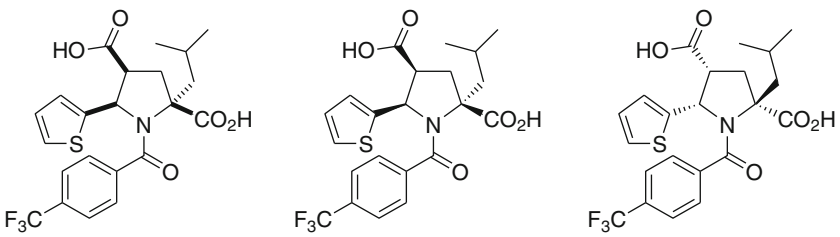

(±)-**6** IC_{50} = 300 nM

(2*S*,4*S*,5*R*)-(+)-**6** IC_{50} = 190 nM

(2*R*,4*R*,5*S*)-(−)-**6** IC_{50} = 18000 nM

Scheme 5

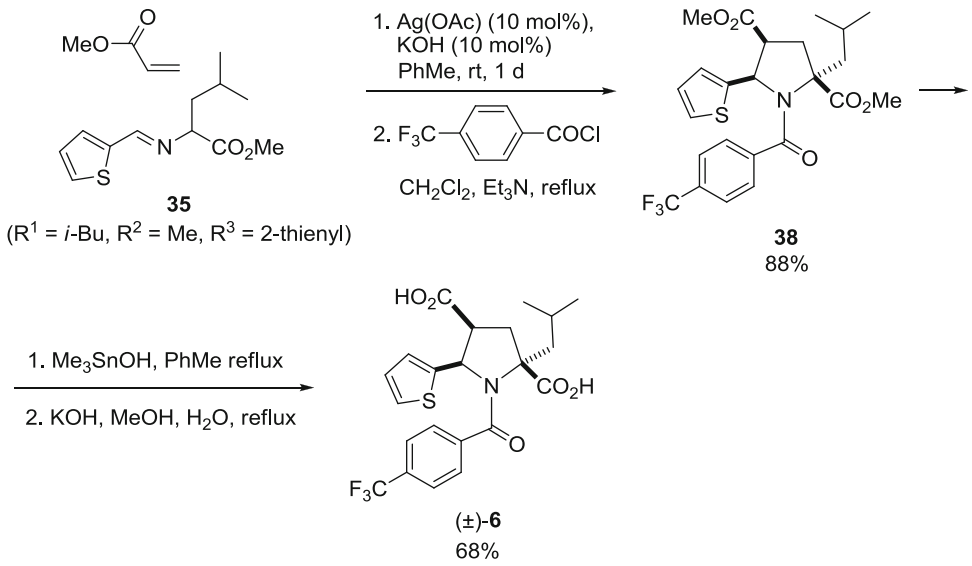

Scheme 6

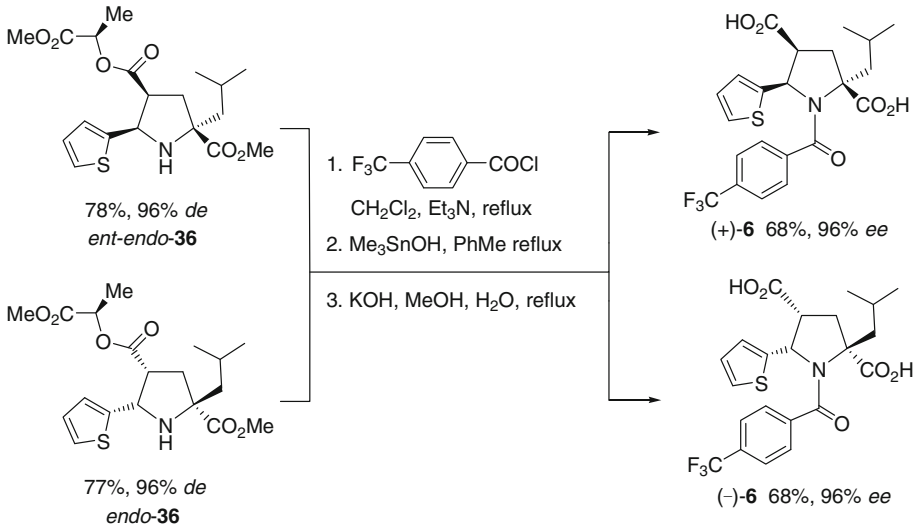

To understand the origins of the excellent regio- and stereocontrol observed by this small chiral environment, DFT calculations were carried out [39]. Based on previous computational work determining that these 1,3-DC occur in a nonconcerted but stepwise mechanism [42], and the structure of the catalytic metal complex (AgOAc in the presence of KOH), four transition states (Fig. 5) were optimized. The absence of an additional ligand/anion to the silver cation (in this case, water is included) promoted a key coordination between the metal and two carboxylate groups which favored the *endo*-approach with the experimentally obtained stereochemistry.

Enantioselective methods

The enantioselective approach is very advantageous because elimination of the chiral auxiliary is not required, and additionally, even a tiny amount of the chiral catalyst is sufficient for the achievement of large enantioselectivity (10 k). Particularly, 1,3-DC of metallo azomethine ylides and alkenes was pioneered by Grigg and coworkers in 1991 using stoichiometric amounts of chiral bases or chiral metal complexes [43]. However, it was only in 2002 that the first substoichiometric catalytic (3 mol%) enantioselective transformation was successfully reported by Zhang and coworkers using a chiral diphosphane/silver(I) complex [44]. At that time, this cycloaddition became a fascinating transformation, and many contributions appeared with outstanding results. Chiral metal complexes, chiral bases, and chiral organocatalysts have all given excellent results, in terms of diastereo- and enantioselectivities, and wider general scope when chiral metallodipoles were generated as intermediates. Based on the previous results obtained with silver(I) [45–48] and copper(I) (for copper(II)-catalyzed 1,3-DC see [49]), a series of catalytic chiral complexes have been

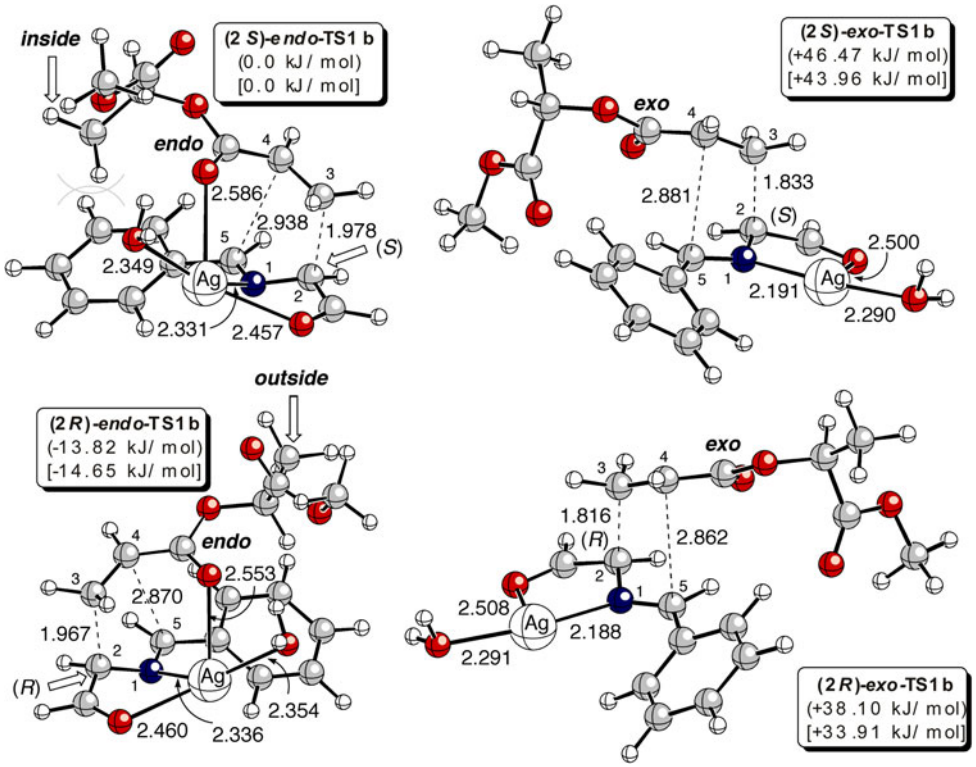

Fig. 5 Relative energies (*in parentheses*) and Gibbs free energies (*in square brackets*) of the four possible transition states for explanation of the observed stereoselectivity (at 298 K)

reported. The most representative recent silver(I) complexes are depicted in Fig. 6, generating the corresponding *endo*-diastereoisomer as major reaction product [50–57], whilst in Fig. 7 the most relevant chiral copper(I) complexes are displayed, which exhibited less well-defined stereoselectivity compared with the silver(I) complexes [58–73]. Other metal cations have also been employed, affording exclusively the *endo*-cycloadducts (Fig. 8) [74–79]. All of these examples were carried out employing α-iminoesters as 1,3-dipole precursors, except for the reactions dealing with azlactones and electrophilic alkenes catalyzed by the chiral **53**-gold(I) complex [78]. Apart from these catalytic enantioselective 1,3-DCs involving α-iminoesters, the generation of stabilized metallo-1,3-dipoles has been achieved starting from α-iminophosphonates using chiral silver(I) complexes [80] and α-iminonitriles employing chiral copper(I) complexes [81].

Organocatalysts have also been successively applied to these cycloadditions [82–97]; however, these and the chiral metal complexes have completely different behaviors concerning the 1,3-dipole and dipolarophile. Organocatalysts, unless their basicity is relatively high, require a highly activated arylideneiminomalonate as 1,3-dipole precursor, and in many cases, its successful enantioselective process is limited to one dipolarophile. In this sense, structural limitations are notable, and there are no wide-

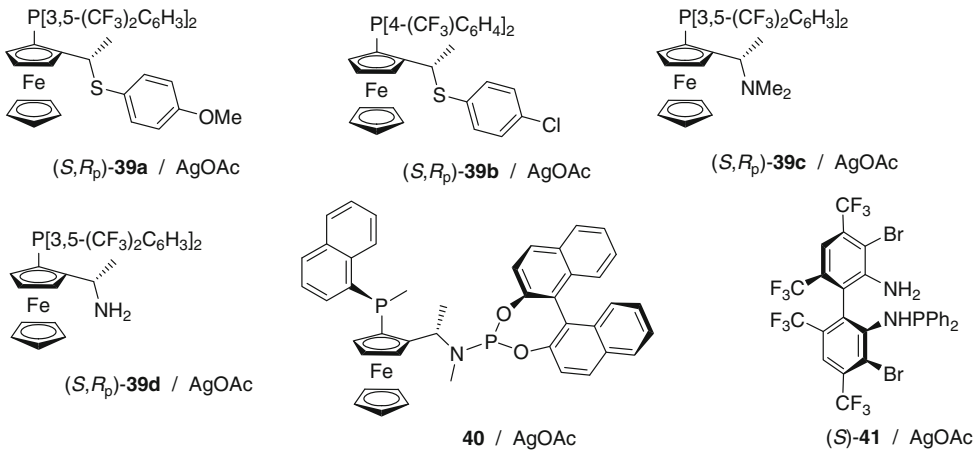

Fig. 6 Chiral ligands/silver salts used to generate chiral Lewis acids employed in enantioselective 1,3-DC of azomethine ylides and dipolarophiles

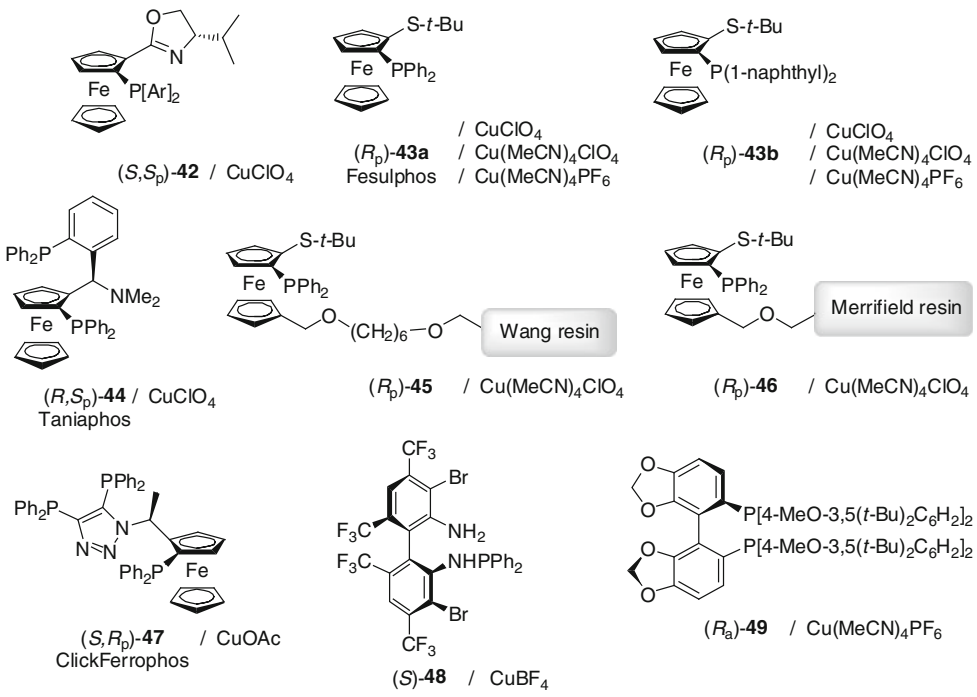

Fig. 7 Chiral ligands/copper(I) salts used to generate chiral Lewis acids employed in 1,3-DC of azomethine ylides and dipolarophiles

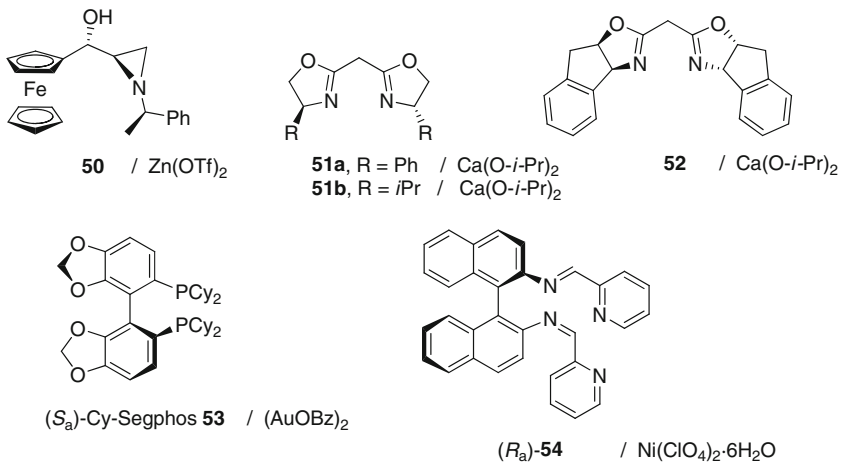

Fig. 8 Chiral ligands/zinc(II), calcium(II), gold(I) or nickel(II) salts used to generate chiral Lewis acids employed in 1,3-DC of azomethine ylides and dipolarophiles

scope transformations at the moment. By contrast, the chiral metal complex-catalyzed enantioselective approach has been much more studied, and the structural limitations are minimal, revealing very interesting broad scope for several chiral metal complexes.

Taking into account all these details, and continuing with our research focused on preparation of antiviral agents, we selected the enantioselective 1,3-DC mediated by a chiral Lewis acid able to afford, in a reliable manner, the relative *endo*-configuration of the target key molecules. Silver(I) salts were the most appropriate at the beginning, and we chose easily available chiral ligands, such as phosphoramidites **42** and **43** and binap **44** (Fig. 9).

Although chiral phosphoramidites **42** and **43** [98] (Fig. 5) have been extensively used in asymmetric hydrogenations and many other transformations, such as allylations, Michael-type additions, and carbonyl addition reactions [99, 100], they were not previously used as ligands in 1,3-DC between azomethine ylides and dipolarophiles. We envisaged that a monodentate ligand would favor the formation of a very highly congested transition state. Initially, optimization of the reaction was carried out at room temperature employing *t*-butyl acrylate and methyl *N*-benzylideneimino glycinates **35** ($R^1 = H$, $R^2 = Me$, $R^3 = Ph$). Employing 5 mol% of catalyst, formed by in situ addition of a 1:1 mixture of phosphoramidite **43** and silver perchlorate, in the presence of triethylamine as organic base (5 mol%), afforded the best enantioselectivity of **45** at −20 °C. The catalysts formed by $AgClO_4$ (5 mol%) and ligand (S_a)-**42** (5 mol%) and triethylamine as

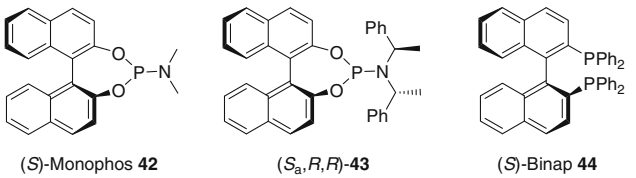

Fig. 9 Chiral ligands employed by Najera's group

base (5 mol%) gave lower *er* of the corresponding cycloadduct. When a 2:1 mixture of $AgClO_4$:(S_a,*R*,*R*)-**43** (5 mol%) was used instead, the *er* was also lower than the result described for the 1:1 mixture. Also, the matching configuration (S_a,*R*,*R*) of the chiral ligand was confirmed for this particular example of cycloaddition [101–103].

In this first enantioselective 1,3-DC of azomethine ylides and alkenes using monodentate ligands, these unknown complexes were characterized by X-ray crystallographic diffraction of monocrystals. Whilst the 1:1 (S_a,*R*,*R*)-**43**:$AgClO_4$ complex formed cross-linked sheets, the 2:1 mixture afforded well-defined crystals (Fig. 10). The formation of these polymeric assemblies is typical of silver(I) complexes, independently of the mono- or bidentate character of the corresponding ligand [104–107].

Electrospray ionization mass spectrometry (ESI–MS) experiments of the 1:1 and 2:1 (S_a,*R*,*R*)-**43**:$AgClO_4$ complexes revealed $[M + 1]^+$ peaks at 646 and 1,187. When equimolar amounts of the 1,3-dipole precursor **35**, triethylamine, and a 1:1 mixture of (S_a,*R*,*R*)-**3**:$AgClO_4$ complex were put together, the ESI experiment revealed a very abundant species with $m/z = 824$ due to the formation of the chiral silver complex-dipole adduct **I** (Fig. 11) and a tiny peak at 1,000 as a result of the combination of two molecules of dipole to the chiral silver complex.

^{31}P NMR ($CDCl_3$, 10 mol% aq. polyphosphoric acid as internal reference) experiments also revealed interesting aspects. Only a wide band centered at 126.9 ppm was observed when a 1:1 mixture of (S_a,*R*,*R*)-**43**:$AgClO_4$ was formed in solution, which corresponded to its polymeric character detected by X-ray diffraction analysis. However, two separated bands were observed at 124.9 and 132.0 ppm in the case of a 2:1 mixture as a consequence of partial disaggregation. Almost complete disaggregation of the polymeric sheets of the 1:1 complex was achieved with addition of 1 equiv. of the 1,3-dipole generated from **35** and triethylamine. The result was transformation of the original ^{31}P NMR band into two perfectly defined doublets at 125.1 ($J_{P–Ag(109)} = 76$ Hz) and 133.61 ppm ($J_{P–Ag(107)} = 73$ Hz), which seems to correspond to the phosphorus atom of complex **I**.

Due to the fact that perchlorates are classified as low-order explosives, the thermal stability of the 1:1 mixture of (S_a,*R*,*R*)-**3**:$AgClO_4$ complex was studied. Thermogravimetric (TG) and differential thermal analysis (DTA) of this

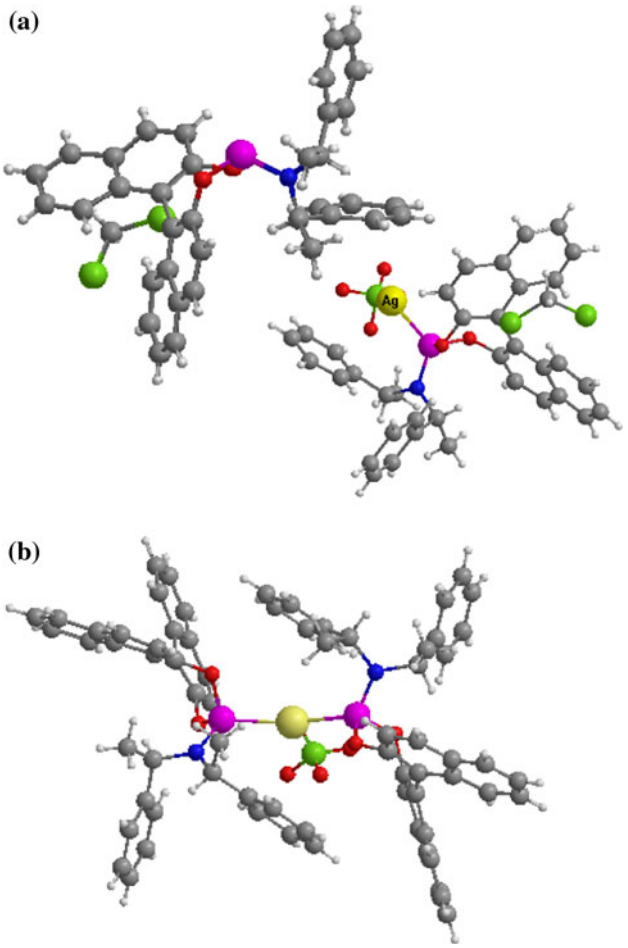

Fig. 10 X-ray diffraction analysis of (**a**) 1:1 **43**-$AgClO_4$ complex and (**b**) 2:1 **43**-$AgClO_4$ complex

Fig. 11 Suggested structure of intermediate complex **I**

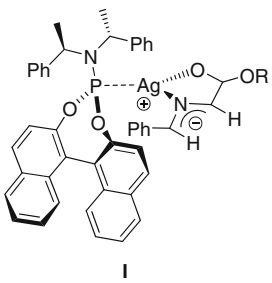

I

complex revealed that loss of water occurred from 50 to 150 °C without any variation of the heat of the system. Exothermic decomposition of the complex started at approximately 200 °C, continuing until 600 °C with noticeable heat liberation.

The scope of the reaction can be observed in the results presented in Scheme 7 and Table 2, operating with methyl or isopropyl iminoesters because *t*-butyl esters did not complete the reaction properly. Isopropyl esters were good starting materials for these enantioselective cycloadditions,

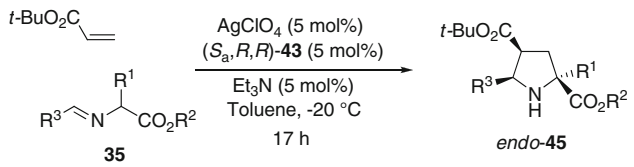

Scheme 7

Table 2 Enantioselective 1,3-DC of iminoesters **35** (R^2 = Me) promoted by 1:1 $AgClO_4$:(S_a,*R*,*R*)-**43** catalytic complex

Entry	R^1	R^2	R^3	Yield (%)[a]	*ee* (%)[b]
1	H	Me	Ph	80	88
2	H	*i*-Pr	Ph	83	99
3[c]	H	Me	2-ClC_6H_4	80	99
4	H	Me	2-Naphthyl	84	91
5	H	*i*-Pr	4-$MeOC_6H_4$	80	98
6	H	*i*-Pr	4-ClC_6H_4	77	94
7	Me	Me	Ph	78	94
8	Bn	Me	Ph	77	98
9	Me	Me	2-Thienyl	70	88
10	*i*-Bu	Me	2-Thienyl	77	82

[a] Isolated yield after purification by flash chromatography

[b] Determined by chiral HPLC columns

[c] Reaction performed with 1,4-diazabicyclo[2.2.2]octane (DABCO) instead of Et_3N

especially when phenyl or 4-substituted aryl iminoglycinates were employed, although methyl esters were more appropriate for the sterically hindered 2-substituted aryl imino groups (Table 2, entries 1–6). For α-substituted 1,3-dipole precursors, the reaction with methyl esters afforded very interesting results. Alanine, phenylalanine, and leucine derivatives afforded high enantioselectivities and good chemical yields (Table 2, entries 7–10), which was a promising result to access finally the desired antiviral framework.

Different dipolarophiles were allowed to react with several iminoesters (Scheme 8). Glycine-derived iminoesters reacted in very good yields with maleimides at higher temperatures (rt or 0 °C), obtaining excellent enantioselectivities of the corresponding cycloadducts **46**. Fumarates, chalcone, and cyclopent-2-enone were very suitable dipolarophiles, employing triethylamine as base at −20 °C. The yields of compounds **47**–**49** were in the range 72–81%, and the enantioselectivities were very large, especially in the examples run with chalcone (>99:1 *er*).

α-Substituted iminoesters derived from alanine and phenylalanine reacted with *N*-methylmaleimide (NMM), furnishing good yields of cycloadducts **46** and high enantiomeric ratios under analogous reaction conditions, the phenylalanine derivative being the less reactive system. Chalcone also reacted with alanine dipole precursor giving good yields of proline derivative **49** (Scheme 8). In all these examples the *endo*:*exo* ratio was higher than 98:2

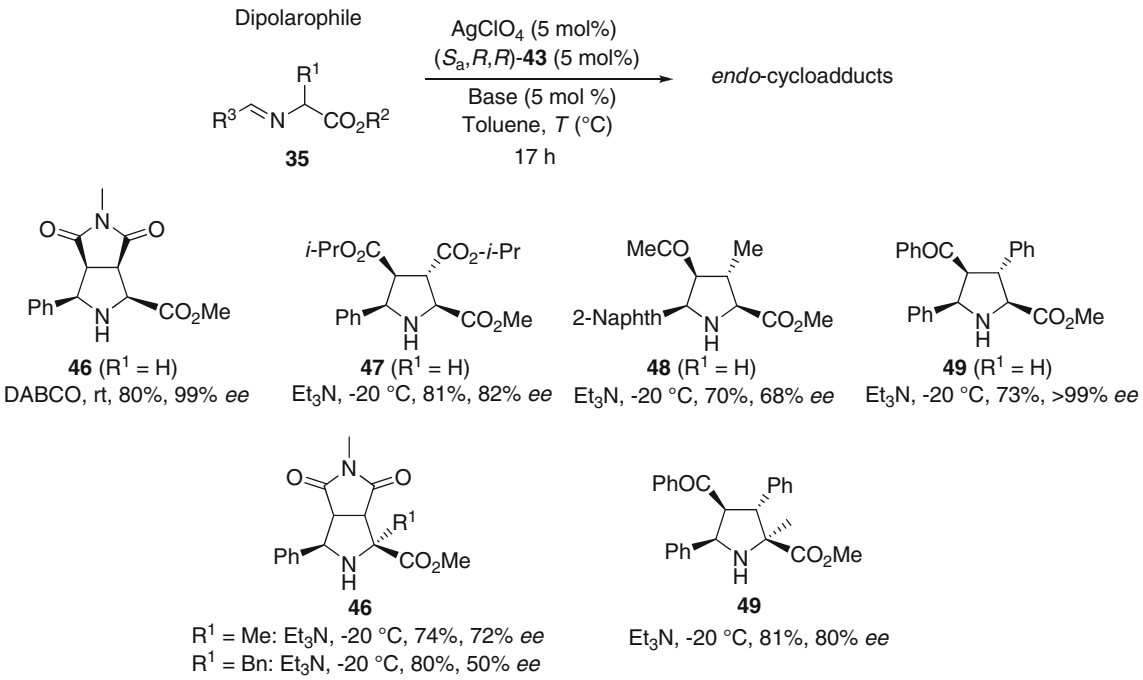

Scheme 8

according to ^{1}H NMR spectroscopy performed on crude reaction products.

As explained in the previous section, enantiomerically pure proline derivative *endo*-**45** (R^1 = *i*-Bu, R^2 = Me, R^3 = 2-thienyl) is the key precursor to a series of antiviral agents that act as inhibitors of the HCV polymerase **6**. The intermediate prolinamide **50** was synthesized in 88% yield (estimated by ^{1}H NMR) from enantiomerically pure *endo*-**45** by a simple amidation reaction with 4-(trifluoromethyl)benzoyl chloride in refluxing dichloromethane during 19 h. The crude product was submitted in a second step to hydrolysis of the *t*-butyl ester with trifluoroacetic acid followed by methyl ester hydrolysis using aqueous solution of KOH in methanol for 16 h. The resulting dicarboxylic acid **6** was finally obtained in 81% yield from compound **50** (50% overall yield from iminoester **35**, Scheme 9). The purity of the antiviral agent was >98%, and only 0.7 ppm silver was present in this sample according to inductively coupled plasma mass spectrometry (ICP-MS) analysis. On the basis of this instrumental technique, purified samples of compound **45** only contained around 4 ppm silver.

Apart from the Lewis acid-catalyzed 1,3-DC, the concept of organocatalysis was applied to the synthesis of **6** using hydroquinine as a chiral base (6 mol%) together with a 3 mol% amount of silver acetate. Although chemical yields were very large, enantioselectivity was moderate (74% *ee*) (Scheme 11, and Table 1, entry 4). In fact, a further 1,1'-binaphthyl-2,2'-dihydrogen phosphate-assisted chiral resolution of **6** was performed to obtain pure compound *endo*-**6** with 99.8% *ee* [90]. Another similar approach, but using chiral calcium complexes, was published after our seminal contribution [76].

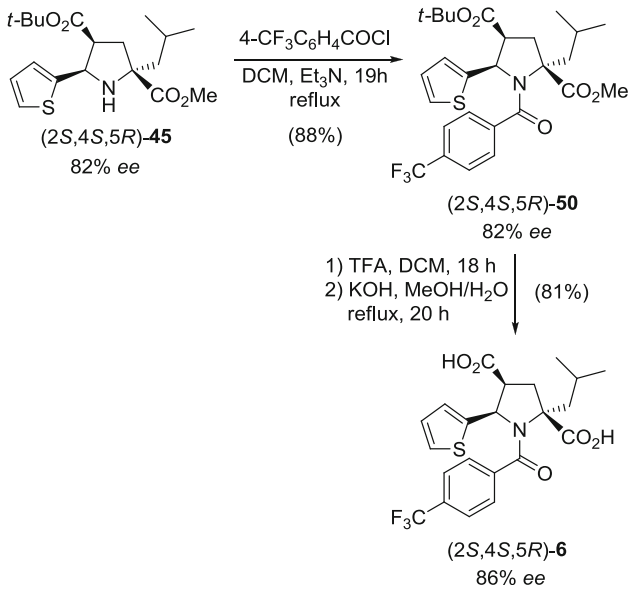

Scheme 9

Calculations were used to locate and characterize the four possible transition structures. The less energetic saddle points are those for the *t*-butoxycarboxyl group in an *endo* relationship with respect to the phenyl group of **35** (R^1 = H, R^2 = Me, R^3 = Ph), being ca. 42 kJ/mol lower than those of their *exo*-analogs.

The two possible *endo*-**TS1** saddle points were much closer in energy (Fig. 12). However, **TS1-SSR** was calculated to be 5.48 kJ/mol lower in energy than **TS1-RRS** (Fig. 12). It is observed that the dihedral angle formed by the two naphthyl groups is ca. 57–58°. In the case of **TS1-SSR**, this leads to blockage of the *Re–Si* face of the dipole, since there is stronger steric congestion between one naphthyl group and the *t*-butyl group of the dipolarophile in **TS1-RRS** (Fig. 12). This results in preferential formation of *endo*-(2*S*,4*S*,5*R*)-**45**, in good agreement with the experimental results.

At that point, the complex formed by chiral phosphoramidite **43** and silver perchlorate (1:1 mixture) was able to promote the already mentioned key step to access enantiomerically enriched first-generation GSK antiviral agents. However, the analogous reaction employing the methyl iminoleucinate derived from 2-thiazolecarbaldehyde and *t*-butyl acrylate afforded very poor enantioselectivity of the key intermediate precursor of chiral pyrrolidine **7**. Alternatively, in parallel studies, we surveyed the applications of chiral binap **44**-silver(I) complexes as catalysts in the enantioselective 1,3-DC with the goal of synthesizing the second-generation agents, and also for improving the enantioselectivity of the first-generation antiviral **6**.

In the publication of the first enantioselective 1,3-DC by Zhang and co-workers, it was described that the combination of (*S*)-binap-AgOAc showed low *ee* when dipoles derived from iminoesters **35** were allowed to react with dimethyl maleate (up to 13% *ee*) [21] or with phenyl vinyl sulfone (up to 26% *ee*) [61, 66]. Fortunately, during our screening process, we realized that the model reaction between iminoester **35** (R^1 = H, R^2 = Me, R^3 = Ph) and NMM in toluene at room temperature afforded exclusively *endo*-cycloadduct **46** (R^1 = H, R^2 = Me, R^3 = Ph) with very good enantioselectivity [108, 109]. After the optimization protocol, we concluded that the best reaction conditions were, once more, toluene as solvent, Et_3N (5 mol%) as base, and a catalytic complex formed by a 1:1 mixture of (*S*)-binap **44** (5 mol%):silver perchlorate (5 mol%) (Scheme 10).

Unlike the previously described new phosphoramidite-silver(I) complexes, the chiral binap-silver(I) complexes were known. Complexes formed from silver triflate and (*R*)- or (*S*)-binap **44** were isolated at different temperatures and further characterized by X-ray diffraction analysis by Yamamoto's group [110]. These studies revealed that a mixture of structures **51**–**53** is in equilibrium at room

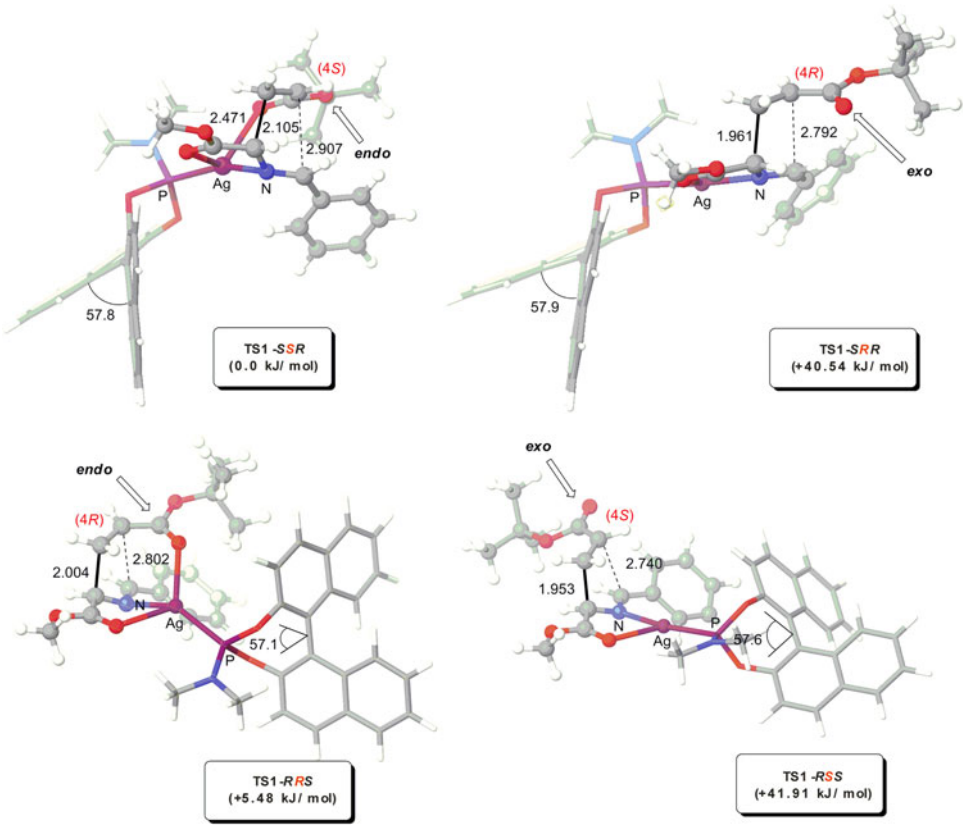

Fig. 12 Chief geometric features saddle relative energies of the four transition structures associated with the first step in the reaction between *t*-butyl acrylate and complex formed by (S_a)-Monophos **42** and imine **35**

Scheme 10

temperature, the 1:1 complex **52** being the most abundant system (Fig. 13).

Equimolar [(*S*)-binap]-$AgClO_4$ and [(*S*)-binap]-AgOAc complexes gave identical chemical yields of product *endo*-**46** (R^1 = H, R^2 = Me, R^3 = Ph) and very high enantioselectivity (>99% and 99% *ee*, respectively). However, the presumed major complex **54** was much more insoluble in toluene than the analog formed by AgOAc. This property allowed separation of the complex **54** from the reaction mixture by simple filtration. Surprisingly, complexes (*R*)- and (*S*)-**44**-$AgClO_4$ exhibited high stability, and any apparent decomposition occurred upon light exposure. Both complexes **54** and **55** (Fig. 14) were prepared and isolated by reaction with 1 and 2 equiv. (*R*)- or (*S*)-binap together with 1 equiv. $AgClO_4$. The mixture was stirred for 1 h at room temperature, and the complexes were obtained in quantitative yield. Complex (*S*)-**54** was further

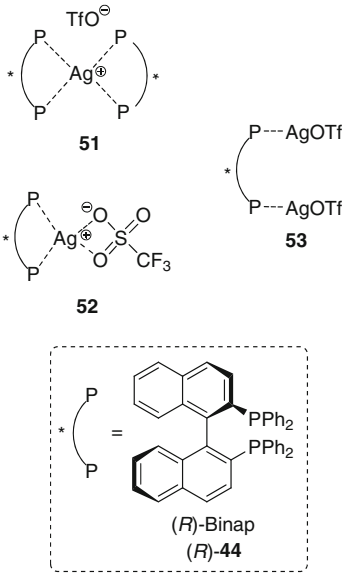

Fig. 13 Identified binap-AgOTf species

characterized by ESI–MS experiments, showing an $[M + 1]^+$ signal at 731 and a tiny one at 1,353. In the case of complex (*S*)-**55**, the same experiment revealed a peak at 1,353 and a very small one at 731. However, these two in situ formed binap complexes **54** and **55** could not be differentiated by ^{31}P NMR spectroscopy. Unfortunately,

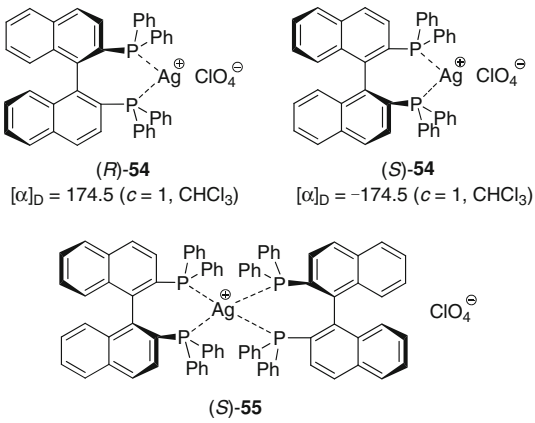

Fig. 14 Chiral binap-silver complexes employed

we could not obtain appropriate crystals for their comprehensive and definitive characterization by X-ray diffraction analysis.

Again, TG and DTA of the stable species **54** were studied. The integrated TG-DTA plot revealed that loss of water of the sample occurred from 50 to 180 °C without variation of the heat of the system. The melting point of this complex **54** was placed in the range 209–211 °C. The three most important exothermic decomposition processes occurred at approximately 300, 550, and 860 °C.

As described above, the easy separation of the most active major complex (*S*)-**54** was a very important feature for application in a larger-scale process. So, in the reaction between iminoester **35** (R^1 = H, R^2 = Me, R^3 = Ph) and NMM in toluene at room temperature a series of cycles were run employing the same catalytic mixture (1:1 **44**-$AgClO_4$), which was recovered and reused without any additional purification (Scheme 10 and Table 3). The reaction shown in Scheme 10 was performed on 1 mmol scale on **35** with 10 mol% catalyst to facilitate its manipulation and successive reutilization. In cycles 1–4 the enantioselectivity was higher than 99% *ee* keeping identical chemical yields (81–91%) (Table 3, entries 1–4). The fifth cycle also afforded the title product *endo*-**46** (R^1 = H, R^2 = Me, R^3 = Ph) in high yield but with slightly lower *ee* (98%) (Table 3, entry 5) due to the effect of possible impurities contained in the catalyst. In all of the five cycles tested, the *endo*:*exo* diastereoselectivity was higher than 98:2 according to ^{1}H NMR experiments.

The scope of the reaction employing different aryl and ester groups at the iminoester **35** structure with assorted dipolarophiles was next investigated. Several ester and aryl groups were appropriate substituents in iminoglycinates **35** to perform 1,3-DC efficiently with maleimides (Scheme 11 and Table 4). Nonsubstituted methyl arylimino-glycinates **35**, derived from benzaldehyde and 2-naphthalenecarbaldehyde, were the best substrates, affording >99% *ee*, rather

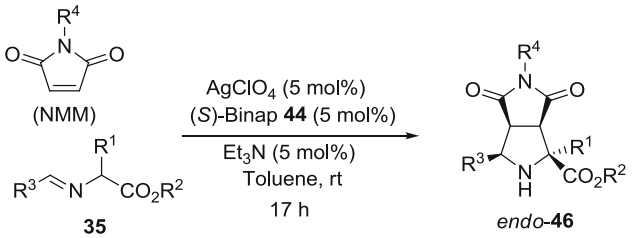

Scheme 11

Table 3 Recycling experiments of 1:1 [(*S*)-binap **44**]:$AgClO_4$ complex

Reaction (mmol)	**35** (mmol)[a]	Recovered catalyst (%)	**46** Yield (%)[b]	**46** *ee* (%)[c]
1	0.100	95	91	>99
1	0.095[d]	93	89	>99
1	0.088[d]	92	91	>99
1	0.081[d]	90	90	99
1	0.073[d]	90	88	98

[a] Recovered after filtration of crude reaction suspension and washed several times with toluene

[b] Isolated yield of compound *endo*-**46** after recrystallization. The conversions were >99%, and the *endo*:*exo* ratios were >98:2 in all of the assayed cycles

[c] Determined by chiral HPLC column (Daicel Chiralpak AS)

[d] Amount recovered from the previous cycle

Table 4 Enantioselective 1,3-DC of iminoesters **35** (R^2 = Me) promoted by 1:1 $AgClO_4$:(*S*)-binap **44** catalytic complex

Entry	R^1	R^2	R^3	R^4	Yield (%)[a]	*ee* (%)[b]
1	H	Me	Ph	Me	90	>99
2	H	Et	Ph	Me	78[c]	91
3	H	*i*-Pr	Ph	Me	80[c]	72
4	H	*t*-Bu	Ph	Me	81[c]	92
5	H	Me	2-Naphthyl	Me	89	>99
6	H	Me	2-ClC_6H_4	Me	82	85
7	H	Me	4-$MeOC_6H_4$	Me	85	99
8	H	Me	2-Thienyl	Me	87	92
9	H	Me	Ph	Et	91	>99
10	H	Me	Ph	Ph	86[c]	62
11	Me	Me	Ph	Me	80	72
12	Bn	Me	Ph	Me	83	64
13	*i*-Bu	Me	2-Thienyl	Me	81	74

[a] Isolated yield after purification by flash chromatography

[b] Determined by chiral HPLC columns

[c] *Endo*:*exo* ratios around 90:20 to 85:25 were observed

than the ethyl, isopropyl, and *t*-butyl esters (Table 4, entries 1–5). In these examples, it was also observed that larger amounts of the *exo* diastereoisomer were formed according to ^{1}H NMR spectroscopy and chiral HPLC columns. In the reaction performed with catalytic complex (*R*)-**44**, the corresponding enantiomer (2*S*,3*R*,4*R*,5*R*)-*endo*-**46** was obtained. More sterically hindered iminoglycinates derived from *ortho*-substituted aromatic aldehydes gave lower enantioselectivity (Table 4, entry 6), even when working at 0 or −20 °C and with bases other than Et_3N, such as 1,8-diazabicyclo[5.4.0]undec-7-ene (DBU) or DIEA. Using Et_3N as base, the imines derived from electron-withdrawing *para*-substituted aromatic aldehydes furnished high enantioselectivity (Table 4, entry 7). Heteroaromatic iminoglycinate bearing a 2-thienyl group furnished *endo*-cycloadduct **46** with 92% *ee* after recrystallization (Table 4, entry 8). Recovery of the complex (*S*)-**54** was successfully attempted in the examples recorded in entries 5, 7, and 9 of Table 4 in 88–93% yield by simple filtration.

Several maleimides were assayed by employing the model reaction described in Scheme 11. *N*-ethylmaleimide afforded similar results of *endo*-**46** to the analog obtained with NMM after 8 h of reaction (Table 4, entry 9). Nevertheless, the bulkier *N*-phenylmaleimide (NPM) furnished lower *ee* (62%) of *endo*-**46** and lower diastereoselectivity (90:10 *endo*:*exo* ratio; Table 4, entry 10).

Next, sterically hindered α-substituted benzaldimino esters were tested as substrates in this 1,3-DC with NMM. Methyl benzylidenealaninate, methyl phenyliminophenylalaninate, and methyl 2-thienyliminoleucinate reacted with NMM under the same reaction conditions at room temperature for 48 h (Table 4, entries 11–13). Cycloadducts *endo*-**46** were diastereoselectively obtained (>98:2 *endo*:*exo* ratio) and with good enantioselectivity (72–76% *ee*).

The absolute configuration of the heterocycle (2*R*,3*S*,4*S*,5*S*)-*endo*-**46** (R^1 = Me, R^2 = Me, R^3 = Ph, R^4 = Me) was determined by X-ray diffraction analysis

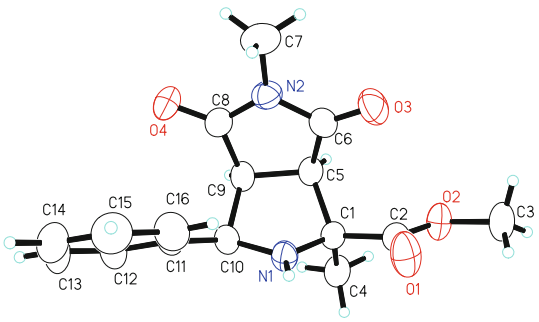

Fig. 15 Oak ridge *thermal ellipsoid* plot (ORTEP) of cycloadduct (2*R*,3*S*,4*S*,5*S*)-*endo*-**46** (R^1 = Me, R^2 = Me, R^3 = Ph, R^4 = Me)

(Fig. 15). 2-Thienyl derivatives can be considered as structurally related precursors of active inhibitors of the virus responsible for hepatitis C.

Dipolarophiles different from maleimides were not appropriate for the particular requirements of this enantioselective 1,3-DC catalyzed by the in situ generated complex (*S*)-**54** (Scheme 12). Acrylates, diisopropyl fumarate, and dimethyl maleate gave very high reaction conversions but the enantioselectivities never exceeded 36% *ee* (Scheme 12) maintaining the high *endo*:*exo* diastereoselectivity.

To obtain better understanding of the behavior of these chiral catalysts, we carried out DFT calculations [109]. The chief geometric features of complex (*S*)-**A** are gathered in Fig. 16. The azomethine ylide part of (*S*)-**A** shows different distances for the two C–N bonds. These distances are compatible with an iminium-enolate structure as shown in Scheme 13, thus anticipating quite asynchronous transition structures in the reaction with the dipolarophile. It is also observed that the metallic center is coordinated to the two phosphorus atoms of the catalysts and to the oxygen and nitrogen atoms of the azomethine ylide. This coordination pattern leads to blockage of the *Re* face of (*S*)-**A** by one of the phenyl groups of the phosphine unit (Fig. 16). This steric hindrance is also generated by the (*S*)-binap moiety, in which the two α-naphthyl subunits form a dihedral angle of ca. 75° (Scheme 14).

The low enantioselectivity in the case of acrylates was a serious drawback, because this is the key step to prepare anti-HCV agents. Taking into account the rejection of perchlorate salts by the industry and the poor coordination of this anion to the metal center, we decided to change to another anion which was weakly bonded to the central metal. According to this experience, we envisaged that the poorly coordinating anion SbF_6^- would modify the chiral domain of the metal complex vacancy, thus allowing the reaction with acrylates [111].

The standard reaction shown in Scheme 10, between methyl benzylideneiminoglycinate **35** (R^1 = H, R^2 = Me, R^3 = Ph) and NMM, was employed for small optimization tests. Initially, the reaction conditions were identical to those previously described for binap-$AgClO_4$-catalyzed 1,3-DC, i.e., 5 mol% catalyst (formed with equimolar amounts of chiral binap and $AgSbF_6$) in toluene at room temperature for 16 h in the presence of Et_3N as base. Both the $AgClO_4$- and $AgSbF_6$-catalyzed reactions gave identical results for the cycloadduct *endo*-**46** (R^1 = H, R^2 = Me, R^3 = Ph) (90% yield, >98:2 *endo*:*exo* ratio, and >99% *ee*).

The reaction was also carried out with the isolated complex formed by the addition of equimolar amounts of (*S*)-binap **44** and $AgSbF_6$, obtaining almost identical results to those described for the reaction carried out with $AgClO_4$. However, this $AgSbF_6$-derived complex became darker

Scheme 12

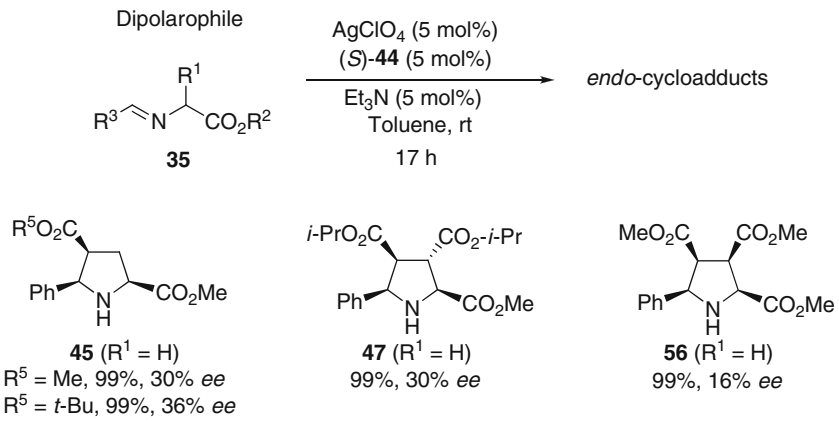

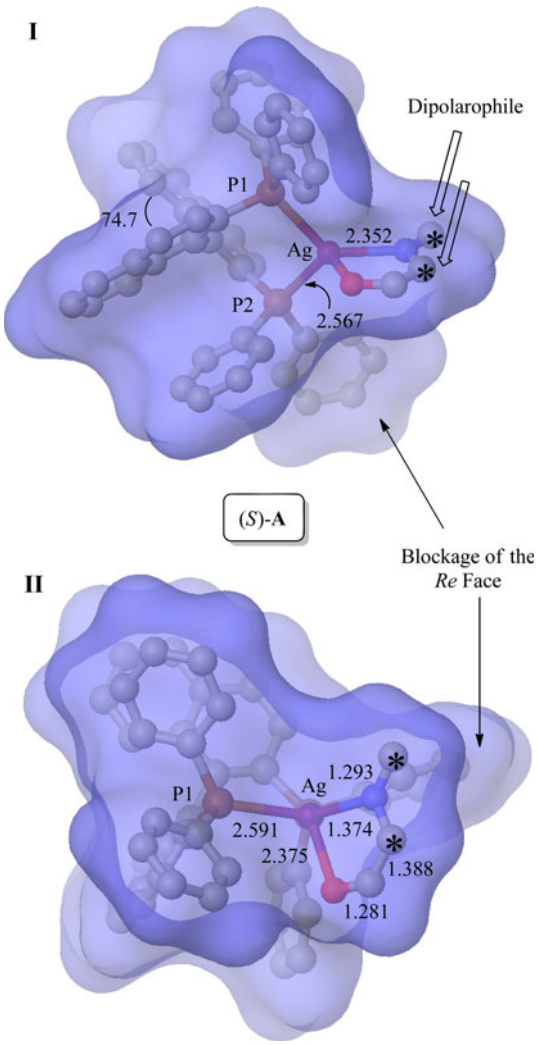

Fig. 16 I: Fully optimized structure (B3LYP/LANL2DZ&6-31G* level) of (*S*)-**A**. The hydrogen atoms have been omitted for clarity. The carbon atoms of the azomethine ylide moiety have been highlighted with *asterisks*. Bond distances and dihedrals are given in Å and degrees, respectively. The molecular surface (probe radius 1.4 Å) is also included. II: View over the *Si* face of (*S*)-**A** along the axis determined by the Ag and P2 atoms

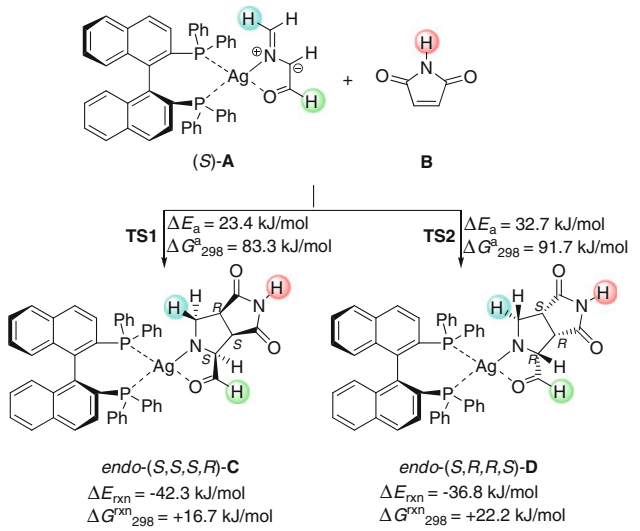

Scheme 13

Scheme 14

upon standing, being much more unstable than the identical complex generated with $AgClO_4$. So, in situ generation of the catalytic complex avoiding light exposure during the whole process was preferred for all the transformations described in this section.

The presumed catalytic monomeric species in solution are identical to those reported previously with different anions [110]. In fact, the 1:1 (*R*)- or (*S*)-binap **44** and $AgSbF_6$ complexes were characterized by ESI–MS exper-

iments and ^{31}P NMR. ESI–MS revealed a $[M + 1]^+$ signal at 731 corresponding to the monomeric 1:1 binap-Ag(I) complex and a tiny one at 1,353 corresponding to the 2:1 binap:$AgSbF_6$. ^{31}P NMR ($CDCl_3$) of 1:1 (*R*)- or (*S*)-binap and $AgSbF_6$ (10% aqueous polyphosphoric acid as internal reference) afforded signals at 15.31 ppm (d, $J_{P\text{-}Ag(109)} = 242$ Hz) (15.26 ppm for binap-$AgClO_4$ complex) and 15.45 ppm (d, $J_{P\text{-}Ag(107)} = 242$ Hz) (15.35 ppm for binap-$AgClO_4$ complex). The absence of non-linear effects (NLE) is another fact supporting the existence of a monomeric species in the enantioselective catalytic process in solution.

In general we could observe that isolated chemical yields of compounds **46** were identical to each other, finding greater enantioselectivity in those reactions promoted by the complex formed by (*S*)-binap and $AgSbF_6$, especially when the aromatic moiety was substituted at different positions or not (Table 5, entries 1–6). Whilst the reaction with NEM does not represent any difference with respect to those results obtained with (*S*)-binap-$AgClO_4$ (Table 5, entry 7), the reaction carried out with NPM was much more enantioselective in the presence of the (*S*)-binap-$AgSbF_6$ complex (82%, versus 62% *ee* obtained with perchlorate-derived chiral complex), and >98:2 *endo*:*exo* ratio was obtained (Table 5, entry 8). Computations revealed the existence of stereoelectronic effects between the phenyl group of the NPM and the binap-$AgClO_4$ catalyst. However, in the case of the binap-$AgSbF_6$-catalyzed process, it seemed that the less coordinating anion decreased the steric congestion of the transition state.

Incorporation of a bulky substituent at the α-position of the 1,3-dipole precursor as occurred in the methyl benzylideneimino-phenylalaninate **35** (R^1 = Ph, R^2 = Me, R^3 = Ph, R^4 = Me) was successfully overcome using the standard reaction conditions. Here, the *endo*-adduct **46** (R^1 = Ph, R^2 = Me, R^3 = Ph, R^4 = Me) was obtained as single enantiomer (99% *ee*) in very good chemical isolated yield (86%). Clearly, this reaction promoted by the (*S*)-binap-$AgSbF_6$ complex improved the results obtained in the reaction performed with the perchlorate salt.

Acrylates, maleates, and fumarates were not suitable dipolarophiles for either the (*S*)-binap **44**-$AgSbF_6$- (<30% *ee* and <40% *ee*, respectively) or for the (*S*)-binap **44**-$AgClO_4$-catalyzed processes, as described above. However, *trans*-1,2-bis(phenylsulfonyl)ethylene **57** afforded very interesting results in the case of *endo*-cycloadducts **58** (Scheme 15). This electrophilic alkene is a synthetic equivalent of acetylene and allows some useful synthetic transformations [65]. The reaction operates under the standard conditions but takes 48 h to complete. This 1,3-DC, not evaluated previously with the chiral perchlorate complex, was performed using both silver salts (Table 6). The four methyl iminoglycinates **35** tested in this reaction under control of the (*S*)-binap-$AgSbF_6$ catalytic complex afforded *endo*-cycloadducts **58** in good chemical yields

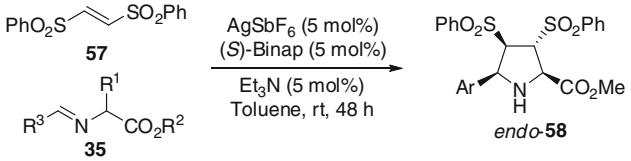

Scheme 15

Table 5 Enantioselective 1,3-DC of iminoesters **35** (R^2 = Me) promoted by 1:1 $AgSbF_6$:(*S*)-binap **44** catalytic complex

Entry	R^1	R^2	R^3	R^4	Yield (%)[a,b,c]	*ee* (%)[c,d]
1	H	Me	Ph	Me	90 (90)	>99 (>99)
2	H	Me	Ph[e]	Me	90 (90)	>99 (>99)
3	H	Me	2-MeC_6H_4	Me	85 (85)	99 (70)
4	H	Me	2-ClC_6H_4	Me	82 (82)	>99[f] (85)[f]
5	H	Me	4-MeC_6H_4	Me	85 (88)	99 (88)
6	H	Me	4-$MeOC_6H_4$	Me	85 (85)	99 (80)
7	H	Me	Ph	Et	84 (91)	99 (99)
8	H	Me	Ph	Ph	86 (86)	82 (62)[g]
9	Ph	Me	Ph	Me	86 (92)	99 (64)

[a] The *endo*:*exo* ratio was always >98:2 (^1H NMR spectroscopy, and chiral HPLC columns)

[b] Isolated after flash chromatography

[c] In parenthesis, the result obtained previously with (*S*)-binap-Ag-ClO_4 complex

[d] Determined by chiral HPLC columns, of the crude product. Identical *ee* was determined after purification

[e] Reaction performed with (*R*)-binap-$AgSbF_6$

[f] Reaction performed at 20 °C

[g] The *endo*:*exo* ratio was approximately 90:10

Table 6 Enantioselective 1,3-DC of iminoesters **35** (R^2 = Me) and disulfone **57**

Entry	R^1	R^2	R^3	Yield (%)[a,b,c]	*ee* (%)[c,d]
1	H	Me	Ph	81 (80)	90 (88)
2	H	Me	Ph[e]	90 (90)	90 (88)
3	H	Me	4-MeC_6H_4	91[f] (85)	88 (28)
4	H	Me	3-Pyridyl	83 (82)	93 (78)
5	H	Me	2-Naphthyl	91[f] (88)	92 (80)

[a] The *endo*:*exo* ratio was >98:2 (^1H NMR spectroscopy and chiral HPLC columns)

[b] Isolated after column chromatography

[c] In parenthesis, the result obtained with (*S*)-binap-$AgClO_4$ complex

[d] Determined by chiral HPLC columns of the crude product. Identical *ee* was determined after purification of **58**

[e] Reaction performed with (*R*)-binap-$AgSbF_6$

[f] Pure crude yields

(80–91%) and very high enantioselectivities (88–92% *ee*) (Table 6). The enantioselectivity was higher than the analogous one exhibited by the chiral silver complex in all of the entries of Table 6, especially in the reaction of *p*-tolyliminoester: 88% versus 28% *ee* (Table 6, entry 3). This is the first synthesis of the disulfonyl *endo*-**58** cycloadducts, whose absolute configuration was determined by nuclear Overhauser effect spectroscopy (NOESY) experiments, and indirectly by comparison of the corresponding HPLC analysis with those described in literature for the *exo*-cycloadducts [65].

The multicomponent version of this transformation was attempted using the best result presented in Tables 5 and 6. Thus, benzaldehyde/NMM or 3-pyridinecarbaldehyde/disulfone **57**, glycine methyl ester hydrochloride, triethylamine (1.05 equiv.), and (*S*)-binap-$AgSbF_6$ (5 mol%) were put together in toluene, and the resulting mixture was allowed to react at rt for 48 h. The results obtained for compound *endo*-**46** (R^1 = H, R^2 = Me, R^3 = Ph, R^4 = Me) or *endo*-**58** (Ar = 3-pyridyl) were impressive (88% yield, >99% *ee*, or 86% yield, 98% *ee*, Scheme 16), taking into account that the analogous reactions in the presence of the (*S*)-binap-$AgClO_4$ complex failed. Although highly activated aminomalonates have been involved as one of the three components of enantioselective organocatalyzed 1,3-DC [85, 93–95], this is the first occasion that a three-component transformation was enantioselectively performed in the presence of a chiral Lewis acid [111].

Evaluating all of these results demonstrates the importance of the anion in this sensitive enantioselective process, which is controlled by many parameters. However, the main conclusion extracted was the impossibility of designing efficiently the key step for the synthesis of antiviral agents employing a combination between the chiral binap **44** ligand and a silver(I) salt. Based on the semiempirical calculations described, and the two images of Fig. 16, it looks like there is not enough space in the enantiodiscrimination domain for accommodation of either bulky substituents of the nitrogen atom in maleimides or the ester groups of the acrylate moiety. The C sp^2 of the ester carbonyl group is not as suitable a coordinating atom as a nitrogen or an oxygen atom belonging to a sulfoxide or a sulfone. In the latter case, the disulfone is much more reactive due to the lower energy of its LUMO. So, it is reasonable to think of a chiral binap **44**-gold(I) complex, as a larger metal cation, able to maintain the same properties of the silver(I) complexes as well as coordination with all these components in an efficient manner.

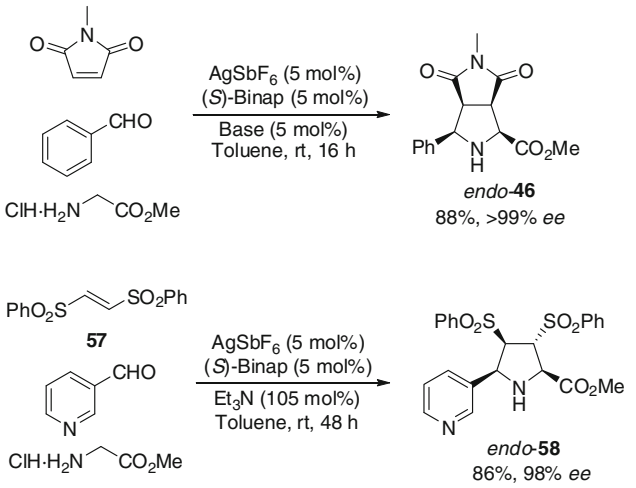

Scheme 16

Toste et al. published the first chiral gold 1,3-DC between mesoionic azomethine ylides (münchnones) with electron-poor alkenes catalyzed by Cy-Segphos$(AuCl)_2$. The reaction afforded in all cases only the *exo*-adduct in high yields and very good enantioselectivities [78]. However, classical 1,3-DC of iminoesters and electrophilic olefins catalyzed by gold complexes was not studied previously [112].

The gold(I) cation has only two coordination sites, and its linear geometry makes asymmetric catalysis extremely difficult. Fortunately, a key to the development of enantioselective gold(I)-catalyzed transformations has been the identification of enantiomerically pure bis(gold)-chiral diphosphine complexes of the form $[(AuX)_2(P–P)^*]$ as catalysts for enantioselective transformations. A clear and recent example of the isolation, identification, and characterization of two chiral binap-gold(I) complexes **59** and **60** (Scheme 17) has been reported by Puddephatt et al. [113]. These complexes were prepared by mixing $(Me_2S)AuCl$ and the corresponding amount of the chiral binap ligand. The resulting gold chloride complexes were treated with different silver salts for 1 h in toluene, and the suspension was filtered through a Celite plug. The remaining solution was evaporated, obtaining **59** or **60** in 89% and 96% yields (Scheme 17).

These cationic complexes were immediately employed without purification in catalytic enantioselective 1,3-DC of the imino ester **35** (R^1 = H, R^2 = Me, R^3 = Ph) and NMM in toluene at rt. The cleanest reaction mixtures and highest conversions were obtained with complexes bearing trifluoroactate as counteranion. When this cycloaddition was performed in the presence of 10 mol% diisopropyl(ethyl)amine (DIPEA) and **59**, product *endo*-**46** (R^1 = H, R^2 = Me, R^3 = Ph) was obtained with high conversion but in racemic form. However, dimeric complexes of type **60** resulted more appropriate. In the case of the chiral complex **60**, 74% *ee* of compound *endo*-**46** (R^1 = H, R^2 = Me, R^3 = Ph) was obtained in the presence of DIPEA, whereas without base a 99% *ee* was

Scheme 17

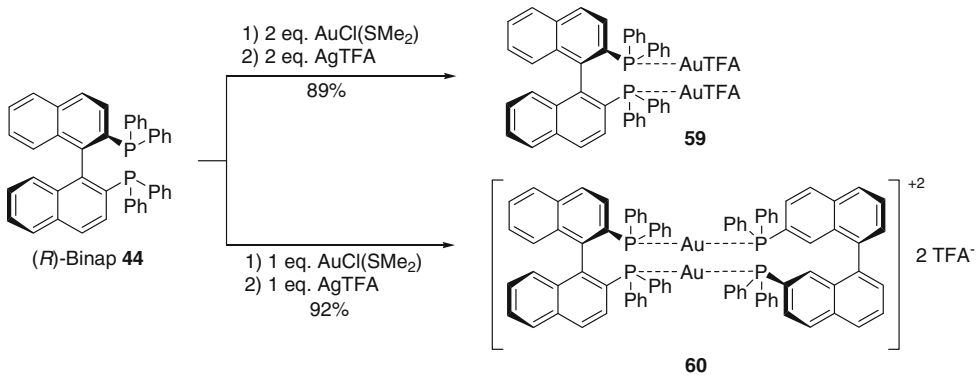

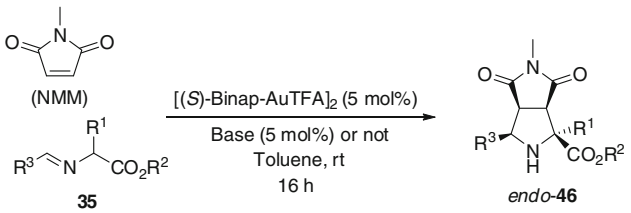

Scheme 18

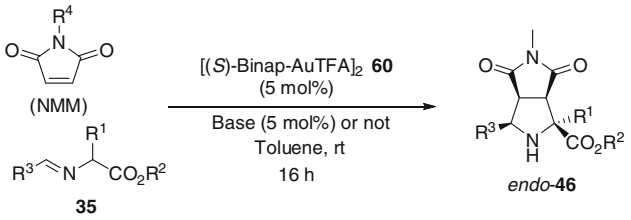

Scheme 19

obtained. The attempt to reduce the catalyst loading to 5 mol% was not successful, as revealed by the lower enantioselectivity (60% *ee*) obtained. In every example, the major cycloadduct obtained was the *endo* (>98:2 *dr*) according to NMR experiments on the crude products. The absolute configuration of proline derivatives **46** was confirmed by comparison of their chiral HPLC columns retention times and specific optical rotations with those described for enantiomerically pure samples.

The scope of this chiral gold(I)-catalyzed enantioselective 1,3-DC was studied using different iminoesters **35** and maleimides under the best reaction conditions described before (Scheme 18). Table 7 presents a comparison between the results obtained with the chiral gold(I) complex **60** and chiral binap-AgOTf complex. In the first examples, reactions of NMM with iminoester **35** (R^1 = H, R^2 = Me, R^3 = Ph) were included, where the absence of base was crucial for achievement of good enantioselectivity (Scheme 19, and Table 7, entries 1 and 2). In the case of employing NEM and NPM, in the absence of base, products **46** (R^1 = H, R^2 = Me, R^3 = Ph, R^4 = Et, Ph)

Table 7 Enantioselective 1,3-DC of iminoesters **35** (R^2 = Me) and maleimides promoted by dimeric catalytic gold(I) complex **60**

Entry	R^1	R^2	R^3	R^4	Base	Yield (%)[a,b,c]	*ee* (%)[c,d]
1	H	Me	Ph	Me	–	90 (90)	99 (99)
2	H	Me	Ph[e]	Me	–	90 (90)	99 (99)
3	H	Me	Ph	Et	–	99 (99)	99 (99)
4	H	Me	Ph	Et	DIPEA	80 (81)	70 (99)
5	H	Me	Ph	Ph	–	81 (81)	80 (*rac*)
6	H	Me	Ph	Ph	DIPEA	89 (89)	64 (*rac*)
7	H	Me	2-Naphthyl	Ph	–	82 (86)	99 (45)
8	H	Me	2-MeC_6H_4	Me	–	90 (86)	99 (50)
9	H	Me	2-ClC_6H_4	Me	–	80 (80)	88 (60)
10	H	Me	4-$MeOC_6H_4$	Me	–	88 (88)	99 (99)
11	Ph	Me	Ph	Me	–	78 (95)	99 (65)

[a] The *endo*:*exo* ratio was always >98:2 (^{1}H NMR spectroscopy, and chiral HPLC columns)

[b] Isolated after flash chromatography

[c] In parenthesis, the result obtained previously with (*S*)-binap-AgTFA complex

[d] Determined by chiral HPLC columns of the crude product. Identical *ee* was determined after purification

[e] Reaction performed with (*R*)-binap

were obtained with higher enantioselectivity than when the reaction was catalyzed by the chiral silver complex (Table 7, entries 3 and 5). However, in the presence of DIPEA (10 mol%), the chiral silver(I)-catalyzed process was more efficient, except in the reaction done with NPM (Table 7, compare entries 4 and 6). In fact, the result obtained when NPM was employed as a dipolarophile (Table 7, entry 5) is particularly noteworthy, because it is the best *ee* (80% *ee*) achieved to date with chiral binap and chiral phosphoramidite ligands. When (S_a)-binap-AgTFA was used as catalyst, racemic product was obtained. For 1,3-DC of other arylideneaminoesters **35** (R^1 = H, R^2 = Me, R^3 = Ar), and maleimides the conversions are identical, independently of the metal cation employed. In the case of 2-naphthyl-derived iminoester the enantioselectivities were very close to the phenyliminoglycinate

ones, but with NPM chiral gold(I) catalysts **2** (X = TFA) (Table 7, entry 7) again was much more efficient generating the highest enantioselectivities. The dipole precursors **35** containing an *ortho*–substituent in the aryl moiety were appropriate sterically hindered starters in the gold(I)-catalyzed 1,3-DC with NMM affording *endo* compounds **46** with 99% and 88% *ee*. In both examples the resulting enantioselectivities induced with the corresponding chiral silver(I) complex were very poor (Table 7, entries 8 and 9). The *para*-substituted methyl iminoglycinates **35** underwent gold(I)- and silver(I)-mediated 1,3-DC, yielding identical enantioselectivities (Table 7, entry 10). The insertion of a substituent at the α-position of the 1,3-dipole precursor was next evaluated. Thus, when methyl benzylideneiminophenylalaninate **35** (R^1 = Ph, R^2 = Me, R^3 = Ar) was allowed to react with NMM under the standard reaction conditions, the reaction performed with the gold(I) complex needed 24 h more than the corresponding reaction using the analogous silver(I) complex to achieve almost total conversion (Scheme 19). The enantioselectivity showed by the (S_a)-binap-AuTFA complex (99% *ee*) was higher than in the example using (S_a)-binapAgTFA (65% *ee*) as catalyst (Table 7, entry 11).

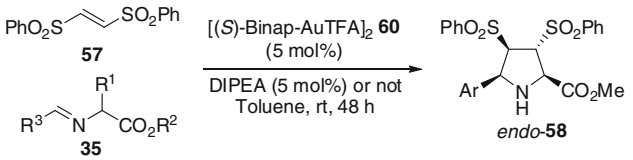

Scheme 20

Table 8 Enantioselective 1,3-DC of iminoesters **35** (R^2 = Me) and disulfone **57** promoted by dimeric catalytic gold(I) complex **60**

Entry	R^1	R^2	R^3	Base	Yield (%)[a,b,c]	*ee* (%)[c,d]
1	H	Me	Ph	DIPEA	81	80 (86)
2	H	Me	Ph	—	74	99 (96)
3	H	Me	2-Naphthyl	DIPEA	91	90 (64)
4	H	Me	2-Naphthyl	—	<40	*rac* (*rac*)
5	H	Me	2-MeOC$_6$H$_4$	DIPEA	80	30 (20)
6	H	Me	2-MeOC$_6$H$_4$	—	<40	40 (20)
7	H	Me	3-Pyridyl	DIPEA	73	96 (92)
8	H	Me	3-Pyridyl	—	73	96 (96)
9	H	Me	4-MeC$_6$H$_4$	DIPEA	91	88 (96)
10	H	Me	4-MeC$_6$H$_4$	—	67	99 (92)

[a] The *endo*:*exo* ratio was always >98:2 (^{1}H NMR spectroscopy, and chiral HPLC columns)

[b] Isolated after flash chromatography

[c] In parenthesis, the result obtained previously with (*S*)-binap-AgTFA complex

[d] Determined by chiral HPLC columns of the crude product. Identical *ee* was determined after purification

According to the previous experience obtained from chiral binap-silver(I) complexes, we also tested the efficiency of the binap-gold(I) trifluoroacetate complexes in the enantioselective cycloaddition of azomethine ylides and *trans*-1,2-bis(phenylsulfonyl)ethylene **57** (Scheme 20 and Table 8). The reaction, performed with 5 mol% gold(I) **60** as catalyst, afforded cycloadducts **58** with non-predictable enantioselectivities in the absence or in the presence of DIPEA (20 mol%) as base. In the case of product **35** (R^3 = Ph), a lower enantiomeric excess was obtained when (S_a)-binap-AgTFA was used as catalyst (Table 8, compare entries 1 and 2). Compound *endo*-**58** (R^3 = 2-naphthyl) was obtained in better enantiomeric excesses in the absence of base (compare entries 3 and 4 in Table 8). The rest of the examples gave the best enantioselectivities in the absence of base and mediated by gold(I) catalyst **60** (Table 8, compare entries 5 and 6, 7 and 8, 9 and 10).

The absolute configuration of the *endo*-cycloadducts was again assigned according to the chiral HPLC column retention times and by comparison of the physical properties of the isolated samples with the properties published in literature for the analogous compounds.

Chiral (R_a)- and [(S_a)-binap-AuTFA] complexes **60** work as multifunctional catalysts acting as Lewis acid (for recent reviews of multifunctional catalysis, see [114–118]) coordinating the dipole and, presumably, the dipolarophile, and as Brønsted base in the enantioselective 1,3-DC of azomethine ylides and maleimides or disulfone **57**.

When other dipolarophiles such as methyl or *t*-butyl acrylate, dimethyl maleate, and diisopropyl fumarate were allowed to react with inimoester **35** (R^1 = H, R^2 = Me, R^3 = Ph) under the optimized reaction conditions, high yields of the corresponding *endo*-cycloadducts were obtained but with very low enantioselectivities. The results obtained with acrylates were very disappointing. In fact, these are the key transformations for achievement of the very promising antiviral agents against the virus responsible for hepatitis C. In spite of this drawback, we decided to start with preparation of **7**, the most potent second-generation antiviral agent. It possesses a sophisticated structural arrangement, bearing a thiazole ring instead of the phenyl group and an isobutyl residue bonded to the α-position of the iminoester. To our surprise, when the general reaction was performed with iminoglycinate **35** (R^1 = *i*-Bu, R^2 = Me, R^3 = 2-thiazolyl) and *t*-butyl acrylate in the presence of triethylamine (10 mol%) and gold(I) catalyst **60** (5 mol%), the resulting cycloadduct *endo*-**45** (R^1 = *i*-Bu, R^2 = Me, R^3 = 2-thiazolyl) was obtained in 79% *ee* (at rt), whilst only 40% *ee* could be achieved by intermediacy of the chiral catalyst (*S*)-binap **44**-AgTFA.

Previously to our work, GSK laboratories obtained this antiviral agent with moderate enantioselectivity (74% *ee*).

In fact, a further 1,1'-binaphthyl-2,2'-dihydrogen phosphate-assisted chiral resolution of **7** was performed to obtain pure compound *endo*-**7** with 99.8% *ee* [90].

With this second objective almost achieved, semiempirical and DFT studies are currently underway to clarify the enantiodiscrimination of the catalytic gold(I) complex **60**. We are also searching for the most convenient route for developing the synthesis of the potent antiviral agent **9**, which constitutes the third challenge of this specific research area.

Conclusions

For diastereoselective synthesis of prolines by silver-catalyzed 1,3-DC of stabilized azomethine ylides derived from iminoesters and acrylate, the corresponding lactate derivative exhibited high yields and diastereoselectivities. However, the enantioselective version of these type of processes using chiral silver complexes has shown greater reaction scope, affording excellent *endo*-diastereoselectivity and high enantioselectivity. Monodentate ligands such as chiral phosphoramidites and silver perchlorate catalyzed the enantioselective synthesis of polysubstituted prolines using different dipolarophiles. In the case of chiral binap and silver perchlorate or silver hexafluoroantimonate, only maleimides and bis-1,2-(phenylsulfonyl)ethylene are appropriate dipolarophiles. Nevertheless, recent experiments with binap-gold trifluoroacetate complexes have shown promising results for the general synthesis of prolines using different types of dipolarophiles and sterically hindered dipole precursors (such as α-substituted iminoesters). These studies focused on synthesis of highly active HCV inhibitors, with the binap-gold complexes being the best catalysts. DFT calculations explained the diastereo- and enantioselectivities observed in these processes, offering a reasonable explanation according to the steric interactions in the transition states.

Acknowledgments This work has been supported by the DGES of the Spanish Ministerio de Ciencia e Innovación (MICINN) (Consolider INGENIO 2010 CSD2007-00006, FEDER-CTQ2007-62771/BQU, and by the Hispano-Brazilian project PHB2008-0037-PC), Generalitat Valenciana (PROMETEO/2009/039), and by the University of Alicante (GITE-09020-UA). We also thank all the participants of this cycloaddition project: M.G. Retamosa, M. Martín-Rodríguez, A. de Cózar, F.P. Cossío, E. Crizanto de Lima, P.R.R. Costa, A.G. Dias, and F.L. Wu.

References

1. Karoyan P, Sagan S, Lequin O, Quancard J, Lavielle S, Chassaing G (2004) Substituted prolines: syntheses and applications in structure-activity relationship studies of biologically active peptides. In: Attanasi OA, Spinelli D (eds) Targets in heterocyclic systems, vol 8. RSC, Cambridge, p 216
2. Calaza MI, Cativiela C (2008) Eur J Org Chem 20:3427
3. Companyó X, Alba AN, Ríos R (2009) Enantioselective synthesis of pyrolidines and piperidines. In: Attanasi OA, Spinelli D (eds) Targets in heterocyclic systems, vol 13. RSC, Cambridge, p 147
4. Pellisier H (2010) Recent developments in asymmetric organocatalysis. RSC, Cambridge
5. Reetz M, List B, Jaroch S, Weinmann R (eds) (2010) Organocatalysis. Springer, New York
6. Nájera C, Sansano JM (2009) Org Biomol Chem 7:4567
7. Nájera C, Sansano JM (2007) Chem Rev 107:4584
8. Huisgen R (1963) Angew Chem Int Ed 10:565
9. Padwa A, Pearson WH (eds) (2003) Synthetic applications of 1, 3-dipolar cycloaddition chemistry towards heterocycles and natural products. Wiley, New Jersey
10. Nair V, Suja TD (2007) Tetrahedron 63:12247
11. Padwa A, Bur SK (2007) Tetrahedron 63:5341
12. Pellissier H (2007) Tetrahedron 63:3235
13. Nájera C, Sansano JM (2003) Curr Org Chem 7:1105
14. Nájera C, Sansano JM (2005) Angew Chem 44:6272
15. Husinec S, Savic V (2005) Tetrahedron Asymmetr 16:2047
16. Pandey G, Banerjee P, Gadre SR (2006) Chem Rev 106:4484
17. Pinho e Melo TMVD (2006) Eur J Org Chem 2873
18. Bonin M, Chauveau A, Micouin L (2006) Synlett 2349
19. Nájera C, Sansano JM (2008) Enantioselective cycloadditions of azomethine ylides. In: Hassner A (ed) Topics in heterocyclic chemistry, vol 12. Springer, New York, p 117
20. Stanley LM, Sibi MP (2008) Chem Rev 108:2887
21. Álvarez-Corral M, Muñoz-Dorado M, Rodríguez-García I (2008) Chem Rev 108:3174
22. Naodovic M, Yamamoto H (2008) Chem Rev 108:3132
23. Nájera C, Sansano JM, Yus M (2010) J Braz Chem Soc 21:377
24. Garner P, Hu J, Parker CG, Youngs WJ, Medvetz D (2007) Tetrahedron Lett 48:3867
25. Chinchilla R, Falvello LR, Galindo N, Nájera C (2001) Eur J Org Chem 3133
26. Sebahar PR, Williams RM (2000) J Am Chem Soc 122:5666
27. Anslow AS, Harwood LM, Phillips H, Lilley IA (1995) Tetrahedron Asymmetr 6:2465
28. Grigg R, Thornton-Pett M, Xu J, Xu LH (1999) Tetrahedron 55:13841
29. Kanemasa S, Hayashi T, Tanaka J, Yamamoto H, Sakurai T (1991) J Org Chem 56:4473
30. Zubía A, Mendoza L, Vivanco S, Aldaba E, Carrascal T, Lecea B, Arrieta A, Zimmerman T, Vidal-Vanaclocha F, Cossio FP (2005) Angew Chem Int Ed 44:2903
31. Williams RM, Fegley GJ (1992) Tetrahedron Lett 33:6755
32. Alcaraz C, Fernandez MD, de Frutos MP, Marco JL, Bernabé M (1994) Tetrahedron 50:12443
33. Pyne SG, Safaei GJ, Javidan A, Skelton BW, White AH (1988) Aust J Chem 51:137
34. Grigg R, Thornton-Pett M, Yoganathan G (1999) Tetrahedron 55:1763
35. Nyerges M, Bendell D, Arany A, Hibbs DE, Coles SJ, Hursthouse MB, Groundwater PW, Meth-Cohn O (1995) Tetrahedron 61:3745
36. Charlton JL, Koh K, Plourde GL (1989) Tetrahedron Lett 30:3279
37. Pham VC, Charlton JL (1995) J Org Chem 60:8051
38. Nájera C, Retamosa MG, Sansano JM (2006) Tetrahedron Asymmetr 17:1985
39. Nájera C, Retamosa MG, Sansano JM, de Cózar A, Cossío FP (2007) Eur J Org Chem 5038

40. Burton G, Ku TW, Carr TJ, Kiesow T, Sarisky RT, Goerke JL, Baker A, Earnshaw DL, Hofmann GA, Keenan RM, Dhanak D (2005) Bioorg Med Chem Lett 15:1553
41. Slater MJ, Amphlett EM, Andrews DM, Bravi G, Burton G, Cheasty AG, Corfield JA, Ellis MR, Fenwick RH, Fernandes S, Guidetti R, Haigh D, Hartley CD, Howes PD, Jackson DL, Jarvest RL, Lovegrove VLH, Medhurst KJ, Parry NR, Price H, Shah P, Singh OMP, Stocker R, Thommes P, Wilkinson C, Wonacott A (2007) J Med Chem 50:897
42. Vivanco S, Lecea B, Arrieta A, Prieto P, Morao I, Linden A, Cossío FP (2000) J Am Chem Soc 122:6078
43. Allway P, Grigg R (1991) Tetrahedron Lett 32:5817
44. Longmire JM, Wang B, Zhang X (2002) J Am Chem Soc 124:13400
45. Chen C, Li X, Schreiber SL (2003) J Am Chem Soc 125:10174
46. Knöpfel TF, Aschwanden P, Ichikawa T, Watanabe T, Carreira EM (2004) Angew Chem Int Ed 43:5971
47. Zheng W, Zhou YG (2005) Org Lett 7:5055
48. Stohler R, Wahl F, Pfaltz A (2005) Synthesis 1431
49. Oderaotoshi Y, Cheng W, Fujitomi S, Kasano Y, Minakata S, Komatsu M (2003) Org Lett 5:5043
50. Zeng W, Zhou YG (2007) Tetrahedron Lett 48:4619
51. Zeng W, Chen GY, Zhou YG, Li YX (2007) J Am Chem Soc 129:750
52. Yu SB, Hu XP, Deng J, Wang DY, Duan ZC, Zheng Z (2009) Tetrahedron Asymmetr 20:621
53. Wang CJ, Xue ZY, Liang G, Lu Z (2009) Chem Commun 45:2905
54. Liang G, Tong MC, Wang CJ (2009) Adv Synth Catal 351:3101
55. Shimizu K, Ogata K, Fukuzawa SI (2010) Tetrahedron Lett 51:5068
56. Oura I, Shimizu K, Ogata K, Fukuzawa SI (2010) Org Lett 12:1752
57. Xue ZY, Liu TL, Lu Z, Huang H, Tao HY, Wang CJ (2010) Chem Commun 46:1727
58. Gao W, Zhang X, Raghunath M (2005) Org Lett 7:4241
59. Yan XX, Peng Q, Zhang Y, Zhang K, Hong W, Hou XL, Wu YD (2006) Angew Chem Int Ed 45:1979
60. Cabrera S, Gómez-Arrayás R, Carretero JC (2007) J Am Chem Soc 127:16394
61. Cabrera S, Gómez-Arrayás R, Martín-Matute B, Cossío FP, Carretero JC (2007) Tetrahedron 63:6587
62. López-Pérez A, Adrio J, Carretero JC (2008) J Am Chem Soc 130:10084
63. Herández-Toribio J, Gómez-Arrayás R, Martín-Matute B, Carretero JC (2009) Org Lett 11:393
64. LLamas T, Gómez-Arrayás R, Carretero JC (2006) Org Lett 8:1795
65. Llamas T, Gómez-Arrayás R, Carretero JC (2007) Synthesis 950
66. Martín-Matute B, Pereira SI, Peña-Cabrera E, Adrio J, Silva AMS, Carretero JC (2007) Adv Synth Catal 349:1714
67. Shi M, Shi JW (2007) Tetrahedron Asymmetr 18:645
68. Fukuzawa S, Oki H (2008) Org Lett 10:1747
69. Wang CJ, Liang G, Xue ZY, Gao F (2008) J Am Chem Soc 130:17250
70. López-Pérez A, Adrio J, Carretero JC (2009) Angew Chem Int Ed 48:340
71. Arai T, Mishiro A, Yokoyama N, Suzuki K, Sato H (2010) J Am Chem Soc 132:5338
72. Zhang C, Yu SB, Hu XP, Wang DY, Zheng Z (2010) Org Lett 12:5542
73. Padilla S, Tejero R, Adrio J, Carretero JC (2010) Org Lett 12:5608
74. Dogan O, Koyuncu H, Garner P, Bulut A, Youngs WJ, Panzner M (2006) Org Lett 8:4687
75. Saito S, Tsubogo T, Kobayashi S (2007) J Am Chem Soc 129:5364
76. Tsubogo T, Saito S, Seki K, Yamashita Y, Kobayashi S (2008) J Am Chem Soc 130:13321
77. Gothelf AS, Gothelf KV, Hazell RG, Jørgensen KA (2002) Angew Chem Int Ed 41:4236
78. Melhado AD, Luparia M, Toste FD (2007) J Am Chem Soc 129:12638
79. Shi JW, Zhao MX, Lei ZY, Shi M (2008) J Org Chem 73:305
80. Yamashita Y, Guo XX, Takashita R, Kobayashi S (2010) J Am Chem Soc 132:3262
81. Robles-Machín R, Alonso I, Adrio J, Carretero JC (2010) Chem Eur J 16:5286
82. Alemparte C, Blay G, Jørgensen KA (2005) Org Lett 7:4569
83. Arai S, Takahasi F, Tsuji R, Nishida A (2006) Heterocycles 67:495
84. Vicario JL, Reboredo S, Badía D, Carrillo L (2007) Angew Chem Int Ed 48:6252
85. Ibrahem I, Ríos R, Vesely J, Córdova A (2007) Tetrahedron Lett 48:6252
86. Xue MX, Zhang XM, Gong LZ (2008) Synlett 691
87. Kudryavtsev KV, Zagulyaeva AA (2008) Rus J Chem 44:378
88. Chen XH, Zhang WQ, Gong LZ (2008) J Am Chem Soc 130:5652
89. Xie J, Yoshida K, Takasu K, Takemoto Y (2008) Tetrahedron Lett 49:6910
90. Agbodjan AA, Cooley BE, Copley RCB, Corfield JA, Flanagan RC, Glover BN, Guidetti R, Haigh D, Howes PD, Jackson MM, Matsuoka RT, Medhurst KJ, Millar A, Sharp MJ, Slater MJ, Toczko JF, Xie S (2008) J Org Chem 73:3094
91. Flanagan RC, Xie S, Millar A (2008) Org Process Res Develop 12:1307
92. Nakano M, Terada M (2009) Synlett 1670
93. Yu L, He L, Chen XH, Song J, Chen WJ, Gong LZ (2009) Org Lett 11:4946
94. Chen XH, Zhang WQ, Gong LZ (2009) J Am Chem Soc 130:5652
95. Chen XH, Wei Q, Luo SW, Xiao H, Gong LZ (2009) J Am Chem Soc 130:13819
96. Iza A, Carrillo L, Vicario JL, Badía D, Reyes E, Martínez JI (2010) Org Biomol Chem 8:2238
97. Li N, Song J, Tu XF, Liu B, Chen XH, Gong LZ (2010) Org Biomol Chem 8:2016
98. Polet D, Alexakis A, Tissot-Croset K, Corminboeuf C, Ditrich K (2006) Chem Eur J 12:3596
99. Minnaard AJ, Feringa BL, Lefort L, de Vries JD (2007) Acc Chem Res 40:1267
100. Teichert JF, Feringa BL (2010) Angew Chem Int Ed 49:2486
101. Nájera C, Retamosa MG, Sansano JM (2008) Angew Chem Int Ed 47:6055
102. Nájera C, Retamosa MG, Sansano JM (2008) Spanish Patent Application: P200800908, May 2008
103. Nájera C, Retamosa MG, Martín-Rodríguez M, Sansano JM, de Cózar A, Cossío FP (2009) Eur J Org Chem 5622
104. Mamula O, von Zelewsky A, Bark T, Bernardinelli G (1999) Angew Chem Int Ed 38:2945
105. Munakata M, Wen M, Suenaga Y, Kuroda-Sowa T, Maekawa M, Anahata M (2001) Polyhedron 20:2037
106. Brandys MC, Puddephatt RJ (2002) J Am Chem Soc 124:3946
107. Reger DL, Semeniuc RF, Elgin JD, Rassolov V, Smith MD (2006) Cryst Growth Des 6:2758
108. Nájera C, Retamosa MG, Sansano JM (2007) Org Lett 9:4025
109. Nájera C, Retamosa MG, Sansano JM, de Cózar A, Cossío FP (2008) Tetrahedron Asymmetr 19:2913
110. Momiyama N, Yamamoto H (2004) J Am Chem Soc 126:5360

111. Martín-Rodríguez M, Nájera C, Sansano JM, Costa PRR, Crizanto-de Lima E, Dias AG (2010) Synlett 962
112. Martín-Rodríguez M, Nájera C, Sansano JM, Wu FL (2010) Tetrahedron: Asymmetry 21:1184 and corringendum 21:2559
113. Wheaton CA, Jennings MC, Puddephatt RJ (2009) Z Naturforsch 64b:1469
114. Ma JM, Cahard D (2004) Angew Chem Int Ed 43:4566
115. Kanai M, Kato N, Ichikawa E, Shibasaki M (2005) Pure Appl Chem 77:2047
116. Kanai M, Kato N, Ichikawa E, Shibasaki M (2005) Synlett 10:1491
117. Shibasaki M, Kanai M, Matsunaga S (2006) Aldrichimica Acta 39:31
118. Walsh PJ, Kozlowski MC (2009) Fundamentals of asymmetric catalysis. University Science Books, New York